UNITED NATIONS UNIVERSITY
GEOTHERMAL TRAINING PROGRAMME
Orkustofnun, Grensásvegur 9,
IS-108 Reykjavík, Iceland

Reports 2007
Number 9

THE LLIXHA ELBASAN HOT SPRINGS IN ALBANIA, STUDY OF TEMPERATURE CONDITIONS AND UTILIZATION CALCULATIONS

Nevton Kodhelaj
Polytechnic University of Tirana
Faculty of Geology & Mining, Department of Energy Resources
Rr. Elbasanit
Tirana
ALBANIA
nevikodheli@yahoo.com

ABSTRACT

The Llixha Elbasan hot springs are among the most important geothermal springs of Albania. Balneological use dates back centuries, but the first modern usage started in 1937. Unfortunately this water hasn't been used for its energetic value yet. The temperature of the water is above 60°C and the flow above 16 l/s, thus direct utilisation is possible, in particular for space heating. Three-dimensional temperature field calculations, a simple study of the dynamics of the hot springs, and engineering calculations on a heating system with heat exchangers are presented here. The results show that the water temperature is expected to be stable, but considerably higher temperatures are expected through welldrilling. The geothermal water of the Llixha hot springs fulfils all the requirements needed for a district heating system in the region.

1. INTRODUCTION

Albania is a small country of only 28,800 km^2 surface area and around 4,500,000 inhabitants, situated in the southwest part of the Balkan Peninsula. Like the other Balkan countries, Albania is located next to the subduction boundary between the African plate and the Eurasian plate. This setting makes the presence of geothermal resources possible. Surface manifestations of geothermal resources are found throughout Albania, ranging from the region of Peshkopia in the northeast, where hot springs with water temperatures of about 43°C and discharge above 14 l/s are found, through the central part of the country with different sources (including the springs of Llixha-Elbasan) with temperatures above 66°C, to the Peri-Adriatic depression (see Figure 1) with a number of wells (drilled for oil and gas research) producing water with temperatures around 40°C at variable flowrates. The thermal waters in Albania are only used for balneology. This form of use dates back to the time of the Roman Empire (e.g. Sarandaporo thermal baths). So far, the geothermal resources have not been utilized for other purposes, such as space heating.

The project presented in this report focuses on the Llixha-Elbasan hot-spring area. Its main purpose is an evaluation of the temperature conditions of the hot springs, and at depth in the reservoir, as well as a preliminary design of a district heating system utilizing the hot springs. Estimated temperature measurements based on different geothermometers indicate that the temperature of the waters in the

formation of the Llixha reservoir may be above 220°C. The reservoir is believed to be at the depth interval of 4500-5000 m. The following is addressed in this report:

- The general geological conditions in the area.
- A review of the theoretical basis of heat transfer.
- Three-dimensional modelling of variations in the temperature conditions in the surface region around the hot-springs, using the finite-element technique.
- Finite-volume modelling of the whole geothermal system down to 5000 m depth, incorporating both thermal convection and conduction, based on simple conceptual boundary conditions.
- A study of the temperature conditions of the hot springs and their up-flow channels on the basis of simple dynamic modelling. Results are compared with the results of geothermometry water temperature estimates.
- A basic engineering design of a district heating network, including tanks and heat exchangers (radiators).

All these aim at demonstrating that the thermal water flowing from the Llixha springs is usable for direct utilisation. This utilisation would mitigate the electricity supply for the region and help improve living conditions for the local community.

FIGURE 1: Map of Albania

2. GEOLOGICAL BACKGROUND OF THE LLIXHA-ELBASAN REGION

The Llixha region is situated southwest of Elbasan. The region is well known for its thermal springs, appreciated since ancient times for their curative properties. A geological map of the region and a representative cross-section (I-I) are presented in Figures 2 and 3.

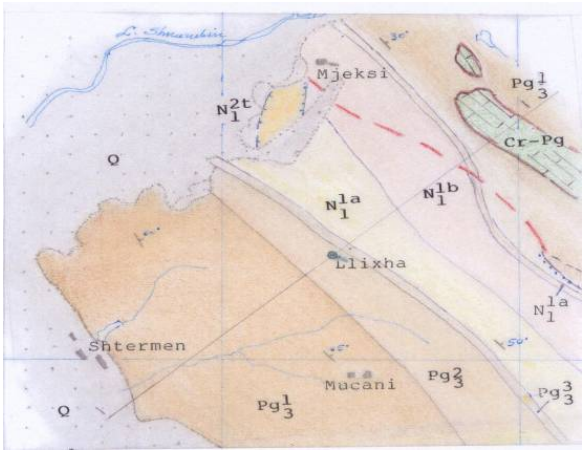

FIGURE 2: Geological map of the Llixha-Elbasan region (Hyseni and Kapllani, 1995)

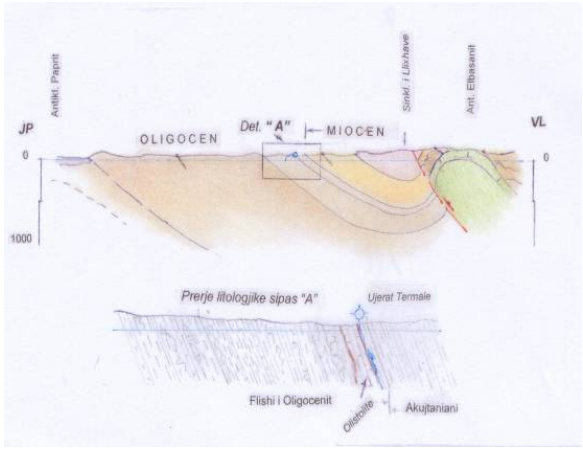

FIGURE 3: Geological cross-section through the area (I-I in Figure 2)

The region under study is south of the Shkumbini river valley. The surface relief increases rapidly up to intermediate elevation (300-500 m). In the western part of the region, a system of hills declines gradually in the Cërriku field. The region has a rich hydrosystem of small streams and many underground water systems. The flowrate for the underground waters varies from 100-200 l/h in Thanë up to 5000 l/h in Tregan. Generally, the formations are composed of flysch with a diverse and chaotic morphology. This is an inhabited area, with small villages clustered around the thermal waters, no more than 2-3 km from each other (Koçiaj, 1989).

The region lies between two tectonic regions; the transversal Vlorë-Elbasan-Dibër and the longitudinal Leskovik-Drini river bay. Both of these connect the lower part of the region with the northern and western parts of the country. In the context of Albanian tectonics, the region represents the western part of the Kruja tectonic zone. The formation represents the Llixha synclinal structure limited by the anticline structures of Elbasan-Valeshit in the east and Papri in the west. The Elbasan-Valeshit structure rises at the surface through the calcareous formation of Creta-Paleogenit, while in Papri the calcareous formations are at greater depth. The orientation of these structures is SW-NE as is the rest of the Albanides structure (Aliaj and Hyseni, 2000).

The formations in the region are mainly composed of flysch (three Oligocene and lower Miocene sections) while calcareous formations with limited surface area are mainly composed of olystolit, through the overlaying terygen rocks. The biggest part is composed of lower Oligocene (Pg_3^1) rocks, consisting of 6 lithological units as shown in Figure 2 (Koçiaj, 2000). The lowest part of the formation is composed of thinner flysch units intercalated by clays and sandstone, while the upper part is composed of thicker flysch with conglomerates.

The lithology of the middle and upper Oligocene formation is mainly flysch with differently shaped packs. Interesting is the lithological evidence of the upper packs of the middle Oligocene where among the flysches calcareous blocks are located with lengths up to 100 m. They are organized in a chain, preserving the general orientation of the other strata. Together with the conglomerate sandstone formation they form a chain alternating in relief. The lithology of the lower Miocene (Acuitan-Burdigalian) deposits is characterized by Margoles alternating with clays-sandstones along with the presence of sandstone-conglomerates.

The Llixha syncline represents a depressed structure with eastern asymmetry filled in the central part with terygen, flysch and molasses deposits. The eastern part is distinguished by an easterly drop. The tectonics put the upper deposits in contact with the lower flysch Oligocene formation and has made the surface intrusion of the Eastern anticline calcareous formations possible. This tectonic layout is regional and includes the western anticline chain of the Kruja tectonic zone (Hyseni and Melo, 2000).

The Llixha system comprises a reservoir which feeds the southern part of the Shkumbini river. The main hydrological characteristic of the region is the presence of several hot springs. Their position is related to the Kruja geothermal zone and they are connected with the calcareous olystolits of the upper Oligocene conglomerate-sandstones. The temperature of the hot springs varies, ranging from 50 to 68°C while flowrates vary from one spring to another, without any seasonal characteristics.

3. HEAT TRANSFER THEORY

3.1 Thermal properties of rocks

The reservoir temperature field and the heat transfer between reservoir rocks and fluid, as well as between different reservoir layers, are highly dependent on the thermal properties of the rocks. In order to determine the equilibrium status (mechanical or thermal), knowledge of three macroscopic properties: pressure P, volume V and temperature T, are needed. The relationship between these

properties $f\ (P,V,T) = 0$, is the so-called equation of state. Determination of temperature as a qualitative property of the system, which determines the thermal equilibrium, only allows a qualitative appreciation of it. In order to determine the temperature in a quantitative way we can use its relationship with the kinetic energy of atoms. It is generally accepted that (Plummer and McGeary, 1988):

$$k \cdot T = \frac{2}{3} E_k = \frac{2}{3} \frac{\overline{mv^2}}{2} = \frac{\overline{mv^2}}{3} \tag{1}$$

where k is the Boltzmann constant, relating energy to temperature Kelvin ($k = 1.380662 \times 10^{-23}$ J/K).

3.2 Specific heat

Specific heat is defined as the energy needed to increase the temperature of a mass by certain amount. Its SI-units are J/kg·K. The specific heat can be measured at constant pressure (C_p) or constant volume (C_v). If the medium is considered to be incompressible, then they are equal (Plummer and McGeary, 1988):

$$C_V = C_P = C(T) \tag{2}$$

In general, $C(T)$ is a function of temperature so that in a given interval the temperature dependence can be approximated as follows:

$$C(T) = C(T_i) + \beta(T - T_i) \tag{3}$$

For saturated rocks at high temperatures, their heat capacity may be calculated by (Plummer and McGeary, 1988):

$$C_R = \frac{M_R}{\rho_m} \tag{4}$$

where

$$M_R = (1 - \Phi)\, M_{ro} + \Phi\,(S_o M_o + S_w M_w) + \Phi S_g \left[f M_g + (1 - f)\left(\frac{\rho_v L_{wv}}{T} + \rho_v C_w \right) \right] \tag{5}$$

and

$$\rho_m = \rho_{ro}\,(1 - \Phi) + \Phi\,(S_o\, \rho_o + S_w \rho_w + S_g\, \rho_g) \tag{6}$$

3.3 Thermal conductivity

Thermal conductivity describes the ability of a material to conduct heat. Consider a wall with an infinite area and of arbitrary material. Its width is one unit and the boundaries of the wall are kept at constant temperatures. The temperature difference is assumed to be one degree. Let's assume that we are able to measure the amount of heat transferred through the wall in one unit of time. This value is the coefficient of thermal conductivity for that material, λ. The units are J/m·s·K. Via experimentation, it has been found that the amount of heat conducted into the wall (ρ_A) is proportional to the area (A), temperature change (ΔT) and the wall thickness (ΔX). This relationship is known as Fourier's law:

$$q = -\lambda \frac{\partial T}{\partial X} \tag{7}$$

The negative sign is used because the heat flows from higher temperature to lower temperature. According to Birch and Clarck (1940), heat conductivity can be approximated by an inversely linear function of temperature:

$$\lambda^{-1} = a_o + a_1 T \tag{8}$$

where a_o and a_1 can be determined for each formation using exponential relationships.

To determine the thermal conductivity of sedimentary rocks at temperatures up to 300°C, the Kutas and Gordienko relationship (Plummer and McGeary, 1988) is used:

$$\lambda_T = \lambda_{20} - (\lambda_{20} - 3.3) e^{0.725 \frac{T-20}{T+130} - 1} \tag{9}$$

where λ_{20} is the thermal conductivity at T=20°C.

3.4 Thermal diffusivity

The thermal diffusivity depends on thermal conductivity and heat capacity and reflects the rate of temperature change in a solid media (Plummer and McGeary, 1988):

$$a = \frac{\lambda}{\rho c} \tag{10}$$

3.5 The geothermal gradient and heat flux

The temperature regime of sedimentary rocks is influenced by several factors: geological, topographical (sedimentary processes, erosion, groundwater movement, etc.), previous climatic changes and the heat flux from depth to the surface. The time-dependent temperature field in 3-D space (*x, y* and *z*) is written as follows:

$$T = T(x, y, z, t) \tag{11}$$

The time variations of temperature are because of climatic changes, which affect the mean annual temperature, and also because of changes in the Earth's heat flux (q).

Various model calculations have shown that the value of q hasn't changed in some millions of years. Climatic changes do not affect temperature at depths greater than 300-500 m. So in an undisturbed area we can neglect time-dependence and rewrite Equation 11 as follows:

$$T = T(x, y, z) \tag{12}$$

It is a well known and accepted fact that temperature increases with depth (except in some rare cases near the oceans or in glacial areas). Temperature conditions are controlled by the geothermal gradient (Γ). In 3-D space, its value is calculated by (Plummer and McGeary, 1988):

$$\Gamma = \sqrt{\Gamma_x^2 + \Gamma_y^2 + \Gamma_z^2} \tag{13}$$

where

$$\Gamma_x = \frac{\partial T}{\partial x} \qquad \Gamma_y = \frac{\partial T}{\partial y} \qquad \Gamma_z = \frac{\partial T}{\partial z} \tag{14}$$

The heat flux density q specifies the amount of heat passing through a unit surface area in one time unit based on the subsurface temperature distribution. For homogenous and isotropic formations the thermal conduction coefficient is constant. The heat flux density q can then be calculated through Fourier's law:

$$\vec{q} = -\lambda grad T = -\lambda \nabla T \tag{15}$$

In anisotropic formations, this relationship takes the form:

$$\vec{q} = (q_x, q_y, q_z) \qquad \nabla T = (T_x,\ T_y,\ T_z) \tag{16}$$

So for homogenous and isotropic formations, the relationship between gradient and heat flux is:

$$q = \lambda \Gamma \tag{17}$$

In order to calculate the heat flux density, it is enough to know the gradient (Γ) and the thermal conductivity of the formation. There are two methods commonly used for this purpose, the so-called interval and the Bullardy methods. In the interval method, the climatic change effect is admitted, and the underground change of heat conductivity, relief change, underground water flows, and the temperature gradient (G) are evaluated; the result was that both gradients are quite similar ($G \approx \Gamma$). In this method, the temperature gradient value is combined with the thermal conductivity of the rock values. Bullardy's method (Plummer and McGeary, 1988) is used only for 1-D heat conduction in layered materials:

$$T(N) = T_0 + q_0 \sum_{i=0}^{N} \frac{\Delta Z_i}{\lambda_i} \tag{18}$$

Following measurements, experiments and several model studies, it was generally accepted that for a very long time the mean values of q over the continents and oceans was unchanged.

The heat content of a geothermal reservoir at a certain moment in time can be determined using the volume model of the heat storage as follows (Frashëri et al., 2004):

$$Q = \{(1-\Phi)\rho_m C + \Phi \rho_w C_w)\}(T_t - T_o) A \Delta Z \tag{19}$$

where C is the specific heat capacity of rock matrix (kJ/kgK)
T_t is the aquifer temperature (°C)
T_o is surface temperature (°C)
ΔZ is thickness of the aquifer (m)
Φ is the porosity

The heat production potential for a single well (with reinjection) is often calculated by the following equation (Frashëri et al., 2004):

$$Q_p = QR_o \tag{20}$$

The extraction coefficient (R_0) can be estimated in several ways, also depending on whether reinjection is applied or not. In the case of reinjection, its value can be estimated by (Frashëri et al., 2004):

$$R_o = 0.33 \frac{T_t - T_r}{T_T - T_o} \tag{21}$$

The heat reserves for production wells can be estimated as follows:

$$Q_{p2} = R_1 Q_p \tag{22}$$

where R_1 is an extraction coefficient for production wells, which can be calculated by:

$$R_1 = \frac{E - I}{Q_p} \qquad \text{with} \begin{cases} E = Q_v (T_t - T_r) \rho_w C_w \Delta t \\ I = \dfrac{I_\$ C}{P} \end{cases} \tag{23}$$

In general, there are only small pressure and flow changes for many geothermal wells and the dependence on rock properties can be estimated by the relationship (Frashëri et al., 2004):

$$Q_w = \frac{2\pi k_v S}{\ln \dfrac{R}{r}} \tag{24}$$

The vertical and horizontal permeability can be determined by (Frashëri et al., 2004):

$$k = \sum_{i=1}^{N} \frac{b_i^2 \Phi_i}{12}; \quad \Phi_i = \sum_{i=1}^{N} b_i D_i \tag{25}$$

The thermal power F_T (MW) from the well can also be estimated by (Frashëri et al., 2004):

$$F_T = Q_{wMAX} \times \{T_{in} - T_{out}\} \times 0.00184 \tag{26}$$

The annual energy production, E_{annual} (J/year) is calculated by (Frashëri et al., 2004):

$$E_{annual} = Q_{vMean} \{T_{in} - T_{oute}\} \times 0.03154 \tag{27}$$

The thermal capacity is then calculated by:

$$K_{Thermal} = \frac{E_{annual}}{F_T} \times 0.03171 \tag{28}$$

3.6 Temperature and lithological profiles

For *N* different layers, with no heat exchange between them except by heat conduction, the product of geothermal gradient and thermal conductivity is constant:

$$\lambda_1 \ \Gamma_1 = \quad \lambda_2 \ \Gamma_2 = \ \ldots\ldots\ldots \quad = \lambda_N \ \Gamma_N \tag{29}$$

This shows that the higher the thermal conductivity for the rocks, the lower the geothermal gradient is. The differential equation for steady vertical conductive heat flow, which gives the relationship between temperature, thermal conductivity $\lambda(T)$ and heat transfer as a function of depth is (Shallo and Daja, 2000):

$$H(Z) + \frac{d}{dZ}\left(\lambda(T)\frac{dT}{dZ}\right) = 0 \tag{30}$$

The boundary conditions are:

$$T_o = T(Z=0); \qquad q_o = \lambda\left(\frac{dT}{dZ}\right)_{Z=0} \tag{31}$$

If $H = H_o$ and $\lambda(T) = \lambda_o/(1+CT)$, then the solution is:

$$T(Z) = \frac{1}{C}\left\{(1 + CT_o)\exp\left[(C/\lambda_o)\left(q_o z - \frac{H_o Z^2}{2}\right)\right] - 1\right\} \tag{32}$$

If $H = H_o e^{\frac{-Z}{D}}$ with $D \approx 10$ km, then:

$$\mid T(Z) = \left(\frac{1}{C}\right)[(1 + CT_o)\exp]\left\{\left(\frac{C}{\lambda_o}\right)\left[H_o D^2\left(1 - \exp\left(-\frac{Z}{D}\right)\right) - H_o DZ + q_o Z\right]\right\} - 1 \mid \tag{33}$$

3.7 The regional characteristics of the heat influx

The most important heat sources in the earth's crust are the radioactive isotopes of Uranium, Thorium, and Potassium. So the crustal thickness and the isotope distribution influence the heat flux from the interior of the Earth. An analytical relationship between this flux and the radioactive heat is (Plummer and McGeary, 1988):

$$q = q_r + DH_o \tag{34}$$

Three empirical equations are used to calculate the radioactive heat, H (μWm^{-3}) (Plummer and McGeary, 1988):

$$H = 10^{-5}\rho\,(9 \le 2\ C_u + 2.56C_{TH} + 3.48\ C_k) \tag{35}$$

$$\ln H = 16.5 - 2.74 v_p \tag{36}$$

$$\ln H = 22.5 - 8.15\rho \tag{37}$$

where C_U, C_{TH}, C_K = Uranium, thorium, natural potassium concentrations;
ρ is the rock density (kg/m^3); and
v_p is the p-wave velocity (m/s).

The measured values of H help in the estimation of H_o by using the above relationships.

3.8 Annual temperature changes

The annual ground temperature change can be simplified by this periodic relationship (Hyseni and Melo, 2000):

$$T(t) = T_o^a + A_o \sin\omega t \tag{38}$$

where $\omega = \frac{2\pi}{P_d}$

The temperature field $T(Z, t)$ at depth in the area of the annual changes is obtained by solving the heat conduction equation for a homogenous semi-infinite medium, with the initial and boundary conditions:

$$\frac{1}{a}\frac{\partial T}{\partial t} = \frac{\partial^2 T}{\partial x^2}; \qquad z > 0 \tag{39}$$

$$T(Z, 0) = T_o + \Gamma_Z\ ;\ T(0, t) = T(t)\ ;\ \ T(0, t) = T_o + \Gamma_Z$$

The solution for this equation is known (Carslaw and Jaeger, 1959):

$$T(Z,t) = T_o + \Gamma_Z + A_o \exp\left(-Z\sqrt{\frac{\omega}{2a}}\right)\sin\left(\omega t - Z\sqrt{\frac{\omega}{2a}}\right) \tag{40}$$

where the temperature amplitude A_z is given by:

$$\frac{A_Z}{A_o} = \exp\left(-Z\sqrt{\frac{\omega}{2a}}\right) \tag{41}$$

Therefore:

$$\frac{A_Z}{A_o} \to 0 \quad for \quad Z \to \infty \qquad \lim_{Z\to\infty} \frac{A_Z}{A_o} = 0 \tag{42}$$

3.9 Heat transfer mechanisms

There are three heat transfer mechanisms; diffusion, convection and radiation. If different parts of a "body" are at different temperatures then there is tendency to equalize them. So part of the energy from the "hot molecules" will be transferred to the "cold" ones. With time this causes the temperatures to equalize. This process is called diffusion. Convection is the process where the energy flows with moving fluid. There are two types of convection: Free, caused by a non-uniform distribution of density resulting in buoyant forces and forced, caused by external factors. Usually they can both occur at the same time, but in different quantities. The relationship shows that the effect of thermal convection is a function of the diffusion/convection processes (Plummer and McGeary, 1988):

$$\gamma_C = \frac{\lambda_e}{\lambda} = 1 + \frac{\lambda_C}{\lambda} \tag{43}$$

In radiation processes heat is released through electromagnetic waves. The amount of energy released per unit area is calculated by:

$$q = \sigma \varepsilon T^4 \tag{44}$$

where $\sigma = 5.67 \times 10^{-8}$ $Wm^{-2}K^{-4}$ and
ε is emissivity.

3.10 The differential equation for heat transfer

This equation is a mathematical expression of the first law of thermodynamics, the energy preservation law. The heat increase of an elementary volume ΔV is equal to the thermal energy which crosses the surface S. A solid medium is considered, which is not generating any energy (so the energy is only flowing through a surface S). The temperature T at a point P (x, y, z) will be a continuous function of the position and time. For a homogenous solid medium, in which the thermal volume heat capacity is independent of temperature, the equation is (conductivity and Plummer and McGeary, 1988):

$$\nabla^2 T = \frac{\partial^2 T}{\partial x^2} + \frac{\partial^2 T}{\partial y^2} + \frac{\partial^2 T}{\partial z^2} = \frac{1}{a}\frac{\partial T}{\partial t} \tag{45}$$

with a = thermal diffusivity of the solid medium.

In polar coordinates $x = r\cos\alpha$; $y = \sin\alpha$, hence:

$$\nabla^2 T = \frac{\partial^2 T}{\partial r^2} + \frac{1}{r}\frac{\partial T}{\partial r} + \frac{1}{r^2}\frac{\partial^2 T}{\partial \theta^2} + \frac{\partial^2 T}{\partial z^2} = \frac{1}{a}\frac{\partial T}{\partial t} \tag{46}$$

Let's assume that at point *P (x, y, z)* the energy input per unit of time and unit of volume is *A(x, y, z, t),* then Equation 45 is rewritten as:

$$\nabla^2 T + \frac{A(x,y,z,t)}{\lambda} = \frac{1}{a}\frac{\partial T}{\partial t} \tag{47}$$

If thermal conductivity depends on position and temperature, the equation can be written as:

$$\rho C \frac{\partial T}{\partial t} = \frac{\partial}{\partial x}\left(\lambda \frac{\partial T}{\partial x}\right) + \frac{\partial}{\partial y}\left(\lambda \frac{\partial T}{\partial y}\right) + \frac{\partial}{\partial z}\left(\lambda \frac{\partial T}{\partial z}\right) + A \tag{48}$$

Its solutions are often relatively simple and can be found for different functional forms of *λ(x, y, z)*. If the thermal properties are temperature dependent, the equation is non-linear and numerical methods need to be used for its solution.

3.10.1 The basic hypothesis

Let's describe mathematically the heat exchange process between flowing fluids in a wellbore with appropriate boundary conditions. Let's assume:

- The formation is homogenous and isotropic;
- The flow is in axial direction only;
- The heat flow is only by conduction;
- There is no radial temperature gradient in the wellbore;
- In the boundary zone of the wellbore the formation temperature is a known function of depth;
- The thermal properties of the fluid and formation are constant;
- The radial temperature in the wellbore is constant;
- The yield from the wells is constant;
- The flow in the wellbore is vertical (1D);
- The vertical heat conduction -is much less than the horizontal one, i.e. negligible;

Wu and Pruess (1990) used a numerical model to verify the last hypothesis. In Figure 4 it can be seen that the ratio between the vertical and horizontal temperature gradients, η, is less than 1%. To determine the value of η, the hypothesis that a constant linear source of heat could simulate the thermal effect of a drilling/production well is used:

$$D = \frac{1}{2u}\int_0^u \left\{ \sqrt{\Pi\left[1 - \Phi\left(\frac{1}{\sqrt{x}}\right)\right]} - \sqrt{x}\left[1 - \exp\left(\frac{-1}{x^2}\right)\right] \right\} dx \tag{49}$$

where Φ is the error function;

$u = \frac{4at}{z^2}$ is dimensionless time;

a is the thermal diffusivity;

z is the depth of the well;

t is the drilling (or production) time; and

$$\{ \lim_{t\to\infty} D = \frac{\sqrt{\Pi}}{2} \approx 0.886 \} \tag{50}$$

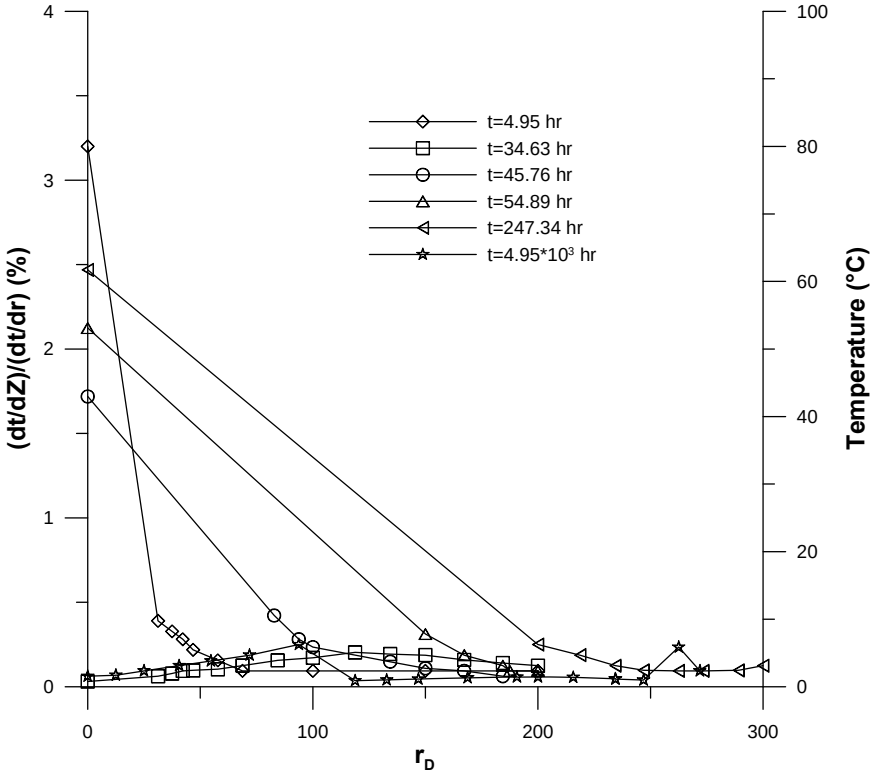

FIGURE 4: The vertical and horizontal temperature gradient ratio (Plummer and McGeary, 1988)

3.11 The Laplace equation

For stable flow through a medium with constant thermal conductivity, without heat production, the form of the heat diffusion equation is:

$$\frac{\partial^2 T}{\partial x^2} + \frac{\partial^2 T}{\partial y^2} + \frac{\partial^2 T}{\partial z^2} = 0 \tag{51}$$

In polar coordinates with $x = r\cos\theta$, $y = r\sin\theta$:

$$\frac{\partial^2 T}{\partial r^2} + \frac{1}{r}\frac{\partial T}{\partial r} + \frac{1}{r^2}\frac{\partial^2 T}{\partial \theta^2} + \frac{\partial^2 T}{\partial z^2} = 0 \tag{52}$$

And for 1-D radial flow:

$$\frac{\partial^2 T}{\partial r^2} + \frac{1}{r}\frac{\partial T}{\partial r} = 0 \tag{53}$$

Using Equation 53, it is possible to calculate the temperature distribution through a cylindrical wall where the heat transfer is only radial in direction. The solution is:

$$T = C_1 \ln r + C_2 \tag{54}$$

where the constants C_1 and C_2 depend on the initial and boundary conditions.

3.12 The Poisson equation

For a medium with constant conductivity and internal heat production the following is used:

$$A(x,y,z) = H/\lambda \tag{55}$$

For stable heat-flow conditions, the diffusion equation is:

$$\frac{\partial^2 T}{\partial x^2} + \frac{\partial^2 T}{\partial y^2} + \frac{\partial^2 T}{\partial z^2} + A(x, y, z) = 0 \tag{56}$$

In polar coordinates, this becomes:

$$\frac{\partial^2 \mathrm{T}}{\partial \mathrm{r}^2} + \frac{1}{\mathrm{r}}\frac{\partial \mathrm{T}}{\partial \mathrm{r}} + \frac{1}{\mathrm{r}^2}\frac{\partial^2 \mathrm{T}}{\partial \theta^2} + \frac{\partial^2 \mathrm{T}}{\partial \mathrm{z}^2} + A(x, y, z) = 0 \tag{57}$$

3.13 Initial and boundary conditions

In order to solve the thermal diffusion equation, let's assume that the formation temperature is a function of position (*x, y, z*) and time (*t*) (Plummer and McGeary, 1988). In addition, initial and boundary conditions must be specified.

A specific moment in time is chosen as the origin of the time coordinate. At that time the temperature distribution is:

$$T(x, y, z, t = 0) = f(x, y, z) \quad \text{or} \quad T(r, \theta, z, t = 0) = f(r, \theta, z) \tag{58}$$

If the radially symmetric case of a flowing wellbore is considered, as an example. After a certain production time the well is shut down. To determine the temperature distribution in the wellbore during the shutdown time, the end of production is considered as the origin of the time coordinate. In this case, the temperature *f(r, z)* must be known, i.e. the initial conditions.

To specify the temperature field of a medium, the boundary conditions must also be known beforehand. Different kinds of boundary conditions can be specified:

- Surface temperature is known, and is constant or a function of position and time, $T = f(x, y, z, t)$;
- The amount of energy flowing through the surface is known:

$$q_s(x,y,z,t) = -\lambda \frac{\partial T}{\partial n} \quad \{\frac{\partial}{\partial n} = \text{the derivation perpendicular to the surface}\} \tag{59}$$

- Linear surface heat flow. In such a case the amount of energy transmitted through a given surface is proportional to the temperature difference between the surfaces and the surroundings.

$$q_s = \alpha(T_s - T_o) \tag{60}$$

where T_s is the surface temperature
T_o is the temperature of the surroundings
α is the heat transfer coefficient, and

$$\{\lim_{\alpha\to\infty} \quad T_s = T_o\} \tag{61}$$

- The connecting surface between two media has the conductivities λ_1 and λ_2, respectively. If T_1 and T_2 are the temperatures of the media, then:

$$T_1|_s = T_2|_s\ ; \qquad -\lambda_1 \frac{\partial T_1}{\partial n}\bigg|_s = -\lambda_2 \frac{\partial T_2}{\partial n}\bigg|_s \tag{62}$$

3.14 Dimensionless parameters

In order to decrease the number of variables involved when solving heat conduction problems, a number of dimensionless parameters are used. Let's consider radial heat flow from a cylindrical source with radius r_c (Plummer and McGeary, 1988):

$$\frac{\partial^2 T}{\partial r^2} + \frac{1}{r}\frac{\partial T}{\partial r} = \frac{1}{a}\frac{\partial T}{\partial t} \qquad\qquad r > r_c \tag{63}$$

With the initial and boundary conditions:

$$T(r, o) = T_o;\ \ T(r_c, t) = T_C;\ T(\alpha, t) = T_o \tag{64}$$

Then the dimensionless parameters for distance, r_D, temperature, T_D and time t_D can be introduced as:

$$r_D = \frac{r}{r_C}, \quad T_D = \frac{T(r,t)}{T_C - T_o}, \quad t_D = \frac{at}{r_{C^2}} \tag{65}$$

Then:

$$\frac{\partial^2 T_D}{\partial r_{D^2}} + \frac{1}{r_D}\frac{\partial T_D}{\partial r_D} = \frac{1}{a} a \frac{\partial T_D}{\partial t_D} = \frac{\partial T_D}{\partial t_D} \tag{66}$$

$$T(r_D, 0) = \frac{T_0}{T_C - T_0}; \quad T(1, t_D) = \frac{T_C}{T_C - T_0} \tag{67}$$

$$T(\alpha, t_D) = \frac{T_0}{T_C - T_0} \tag{68}$$

4. THERMODYNAMICS OF THE HOT SPRINGS

4.1 Temperature field modelling

In order to create a physical model to enable the stable state of heat flow through a formation to be studied, the analogy principle may be used. It is assumed that n dimensionless parameters I_1, ... I_n describe the heat conditions in the formation and surroundings. In such a case, the model results should be expressed as n dimensionless parameters I'_1, ... I'_n. The conditions that must be fulfilled in order to use the model in a real reservoir are $I_1 = I'_1$, ... $I_n = I'_n$. For stable heat transmission, the analogy with the electrostatic field can be used. For the 2D case and with the thermal conductivity as $\lambda=\lambda(x,y)$, the boundary conditions are:

$$T(z_1,x)=T_1,\ T(z_2,x)=T_2,\ -l \le x \le l\ ; \quad \frac{\partial T(z,x)}{\partial x}\Big|_{-l} = \frac{\partial T(z,x)}{\partial x}\Big|_{l} = 0 \tag{71}$$

TABLE 1: The analogy between different physical fields (based on Plummer and McGeary, 1988)

Hydrodynamics	**Heat transfer**	**Electrostatics**	**Electricity transmission**
Pressure P	Temperature T	Electrostatic potential Φ	Potential U
Pressure gradient (negat.) $-\nabla P$	Temperature gradient (negat.) $-\nabla T$	Field vector $E = -\nabla \Phi$	Potential gradient (negat.) $-\nabla U$
Permeability/viscosity k/μ	Thermal conductivity λ	Dielectric constant $\varepsilon/4\pi$	Specific resistance ρ
Velocity vector $\vec{v} = -\frac{k}{\mu}\nabla p$ (Darcy law)	Heat amount transfer. $\vec{q} = -\nabla T$ (Fourier law)	Dielectric displ. $\frac{\varepsilon}{4\pi}\vec{E} = -\frac{\varepsilon}{4\pi}\nabla\Phi$ (Maxwell law)	Current $\vec{I} = -\nabla U$ (Ohm law)
Isobaric surface $p=C$	Isothermal surface $T=C$	Surface with electrostatic potential $\Phi=C$	Surface with potential $s=C$
Impermeable layer $\frac{\partial p}{\partial n} = 0$	Split surface $\frac{\partial T}{\partial n} = 0$	Force line $\frac{\partial \Phi}{\partial n} = 0$	Potential line $\frac{\partial U}{\partial n} = 0$

In Table 1, a summary of the analogies between hydrodynamic, heat transfer, electrostatic and electricity transmission fields is presented. As can be seen from Table 1, temperature change ΔT is analogous to the potential difference ΔU. Assuming a unit length, l_s , the dimensionless coordinates are:

$$x' = \frac{x}{l_s}; z' = \frac{z}{l_s}; z_1' = \frac{z_1}{l_s}; z_2' = \frac{z_2}{l_s};\ l' = \frac{l}{l_s} \tag{72}$$

The relationship $\lambda = \lambda(x,z)$ is analogous with $\rho = \rho(x,z)$. Particular care should be used in unstable field modelling. Considering the hydrodynamics analogy with the thermal one, in particular the transitory flows of an incompressible fluid through a porous medium, then the main characteristics of this regime are the high value of the hydraulic diffusivity (Aliaj and Hyseni, 1996):

$$\eta = \frac{k}{\Phi\, c_t \mu} \tag{73}$$

Its thermal field analogue is the thermal diffusion coefficient (a). The analogies principle can only be used in a case where the dimensionless times are equal. In thermal field modelling, the fact that the temperature is not affected by surface topography and groundwater flow is very important. To determine the boundary conditions, temperatures maps at depth are widely used (Čermak and Haenel, 1988).

4.2 The unstable temperature field

Before starting investment in a geothermal project, the stability of the temperature field involved, in space and time, needs to be confirmed as well as the project's overall sustainability. The methods that can be used to answer such questions are numerous, but here we will apply the finite element method (Osmani, 1997). Considering the differential equation:

$$\frac{\partial}{\partial x}(k_x \frac{\partial T}{\partial x}) + \frac{\partial}{\partial y}(k_y \frac{\partial T}{\partial y}) + \frac{\partial}{\partial z}(k_z \frac{\partial T}{\partial Z}) + q(x,y,z) - c\frac{\partial T}{\partial t} = 0 \tag{74}$$

The functional of this equation is (Osmani, 1997):

$$X = X_v + X_r = \iiint_{\Omega}\left[\frac{k_x}{2}\left(\frac{\partial T}{\partial x}\right)^2 + \frac{k_y}{2}\left(\frac{\partial T}{\partial y}\right)^2 + \frac{k_z}{2}\left(\frac{\partial T}{\partial z}\right)^2\right]dxdydz + \iiint_{\Omega}\left(q - c\frac{\partial T}{\partial t}\right)dxdydz \qquad (75)$$

Let's divide this functional into two parts:

$$X_v = \iiint_{\Omega}\left[\ \frac{k_x}{2}\left(\frac{\partial T}{\partial x}\right)^2 + \frac{k_y}{2}\left(\frac{\partial T}{\partial y}\right)^2 + \frac{k_z}{2}\left(\frac{\partial T}{\partial z}\right)^2\ \right]dxdydz;\ \ X_r = \iiint_{\Omega}\left(q - c\frac{\partial T}{\partial t}\right)dxdydz \qquad (76)$$

The initial conditions are: $T(x,y,z,t{=}0) = f(x,y,z)$ and the boundary conditions are (Osmani, 1997):

$$k_x\frac{\partial T}{\partial x}l + k_y\frac{\partial T}{\partial y}m + k_z\frac{\partial T}{\partial z}n + q + \alpha T = 0$$

where m, n and l are the heading cosines of a vector perpendicular to the surface of volume Ω;
q = heat flow density of surface hot springs [$q = \alpha(T\text{-}T_g)$]; with
α = convection heat transfer coefficient.

This is a 3-D temperature field problem. To integrate this equation it is assumed that the time interval $(t,t+\Delta t)$ leads into dT/dt = C ($T_{i=}$ temperature values in the nodes I = 1, 4).

$$\frac{\partial X}{\partial T_i} = \frac{\partial X_v}{\partial T_i} + \frac{\partial X_r}{\partial T_i};\ \ T = \frac{1}{6\Delta}\left[N_1N_2N_3N_4\right]\begin{Bmatrix}T_1\\T_2\\T_3\\T_4\end{Bmatrix}\ where\ N_i(x,y,z) = (\ a_i + b_ix + c_iy + d_iz);\ i = \overline{1,4} \qquad (77)$$

The partial derivatives of the functional can be calculated as follows:

$$\frac{\partial X}{\partial T_i} = \begin{Bmatrix}\frac{\partial X}{\partial T_1}\\ \frac{\partial X}{\partial T_2}\\ \frac{\partial X}{\partial T_3}\\ \frac{\partial X}{\partial T_4}\end{Bmatrix} = \left\langle \begin{matrix} \frac{k_x}{36\Delta}\begin{vmatrix} b_1^2 & b_1b_2 & b_1b_3 & b_1b_4\\ b_2b_1 & b_2^2 & b_2b_3 & b_2b_4\\ b_3b_1 & b_3b_2 & b_3^2 & b_3b_4\\ b_4b_1 & b_4b_2 & b_4b_3 & b_4^2\end{vmatrix} + \frac{k_y}{36\Delta}\begin{vmatrix} c_1^2 & c_1c_2 & c_1c_3 & c_1c_4\\ c_2c_1 & c_2^2 & c_2c_3 & c_2c_4\\ c_3c_1 & c_3c_2 & c_3^2 & c_3c_4\\ c_4c_1 & c_4c_2 & c_4c_3 & c_4^2\end{vmatrix} + \\ + \frac{k_z}{36\Delta}\begin{vmatrix} d_1^2 & d_1d_2 & d_1d_3 & d_1d_4\\ d_2d_1 & d_2^2 & d_2d_3 & d_2d_4\\ d_3d_1 & d_3d_2 & d_3^2 & d_3d_4\\ d_4d_1 & d_4d_2 & d_4d_3 & d_4^2\end{vmatrix} \end{matrix} \right\rangle \begin{Bmatrix}T_1\\T_2\\T_3\\T_4\end{Bmatrix} - \qquad (78)$$

$$+\begin{vmatrix} \iiint_{\Omega}N_1^2dxdydz & \iiint_{\Omega}N_1N_2dxdydz & \iiint_{\Omega}N_1N_3dxdydz & \iiint_{\Omega}N_1N_4dxdydz\\ \iiint_{\Omega}N_2N_1dxdydz & \iiint_{\Omega}N_2^2dxdydz & \iiint_{\Omega}N_2N_3dxdydz & \iiint_{\Omega}N_2N_4dxdydz\\ \iiint_{\Omega}N_3N_1dxdydz & \iiint_{\Omega}N_3N_2dxdydz & \iiint_{\Omega}N_3^2dxdydz & \iiint_{\Omega}N_3N_4dxdydz\\ \iiint_{\Omega}N_4N_1dxdydz & \iiint_{\Omega}N_4N_2dxdydz & \iiint_{\Omega}N_4N_3dxdydz & \iiint_{\Omega}N_4^2dxdydz\end{vmatrix}\begin{Bmatrix}\frac{\partial T_1}{\partial t}\\ \frac{\partial T_2}{\partial t}\\ \frac{\partial T_3}{\partial t}\\ \frac{\partial T_4}{\partial t}\end{Bmatrix} - \frac{Q\Delta}{4}\begin{Bmatrix}1\\1\\1\\1\end{Bmatrix} = \begin{Bmatrix}0\\0\\0\\0\end{Bmatrix}$$

The following replacements are done:

$$\left\langle \frac{k_x}{36\Delta}\begin{vmatrix} b_1^2 & b_1b_2 & b_1b_3 & b_1b_4 \\ b_2b_1 & b_2^2 & b_2b_3 & b_2b_4 \\ b_3b_1 & b_3b_2 & b_3^2 & b_3b_4 \\ b_4b_1 & b_4b_2 & b_4b_3 & b_4^2 \end{vmatrix} + \frac{k_y}{36\Delta}\begin{vmatrix} c_1^2 & c_1c_2 & c_1c_3 & c_1c_4 \\ c_2c_1 & c_2^2 & c_2c_3 & c_2c_4 \\ c_3c_1 & c_3c_2 & c_3^2 & c_3c_4 \\ c_4c_1 & c_4c_2 & c_4c_3 & c_4^2 \end{vmatrix} + \right.$$
$$\left. + \frac{k_z}{36\Delta}\begin{vmatrix} d_1^2 & d_1d_2 & d_1d_3 & d_1d_4 \\ d_2d_1 & d_2^2 & d_2d_3 & d_2d_4 \\ d_3d_1 & d_3d_2 & d_3^2 & d_3d_4 \\ d_4d_1 & d_4d_2 & d_4d_3 & d_4^2 \end{vmatrix} \right\rangle = [H] \tag{79}$$

$$\left\| \begin{matrix} \iiint_\Omega N_1^2\,dxdydz & \iiint_\Omega N_1N_2\,dxdydz & \iiint_\Omega N_1N_3\,dxdydz & \iiint_\Omega N_1N_4\,dxdydz \\ \iiint_\Omega N_2N_1\,dxdydz & \iiint_\Omega N_2^2\,dxdydz & \iiint_\Omega N_2N_3\,dxdydz & \iiint_\Omega N_2N_4\,dxdydz \\ \iiint_\Omega N_3N_1\,dxdydz & \iiint_\Omega N_3N_2\,dxdydz & \iiint_\Omega N_3^2\,dxdydz & \iiint_\Omega N_3N_4\,dxdydz \\ \iiint_\Omega N_4N_1\,dxdydz & \iiint_\Omega N_4N_2\,dxdydz & \iiint_\Omega N_4N_3\,dxdydz & \iiint_\Omega N_4^2\,dxdydz \end{matrix} \right\| = [P]$$

$$\frac{q_i\Delta}{4} = [F]$$

where $[H]$ = Matrix of conductivity of the thermal field;
$[P]$ = Matrix of instability of the thermal field; and
$[F]$ = Source vector.

After these replacements the definitive form of Equation 78 becomes:

$$[H]|T| + [P]\frac{\partial T}{\partial t} - |F(t)| = 0 \tag{80}$$

This matrix equation can be solved step by step. Expanding it as a Taylor series we obtain:

$$\begin{aligned} T(t+\Delta t) &= T(t) + \frac{\Delta t}{1!}\frac{\partial T}{\partial t} + \frac{\Delta t^2}{2!}\frac{\partial^2 T}{\partial t^2} \\ \frac{\partial}{\partial t}T(t+\Delta t) &= \frac{\partial T}{\partial t} + \frac{\Delta t}{1!}\frac{\partial^2 T}{\partial t^2} \\ \frac{\partial}{\partial t}T(t+\Delta t) &= \frac{2}{\Delta t}\left[T(t+\Delta t) - T(t)\right] - \frac{\partial T(t)}{\partial t} \end{aligned} \tag{81}$$

At times t and $t+\Delta t$, this equation is written:

$$[H]T(t) + [P]T(t) + [P]\frac{\partial T(t)}{\partial t} - F(t) = [0] \tag{82}$$

$$[H]T(t+\Delta t) + [P]T(t+\Delta t) + [P]\frac{\partial T(t+\Delta t)}{\partial t} - F(t+\Delta t) = [0] \tag{83}$$

$$\left\{[H]+\frac{2}{\Delta t}[P]\right\}\{T(t+\Delta t)\}+\left\{[H]-\frac{2}{\Delta t}[P]\right\}\{T(t)\}-\{F(t+\Delta t)+F(t)\}=\{0\} \tag{84}$$

The temperature vector at time t will help to find the temperature at time ($t+\Delta t$), which will help to find the temperature at time ($t+2\Delta t$) and so on (see Appendix I).

4.3 Pipe flow with heat addition

The flow to hot springs can often be modelled by flow in a pipe surrounded by rock. If the heat balance in a thin cylindrical shell of fluid in the pipe is considered, as shown in Figure 5, the thickness of the shell is δr and the length δx.

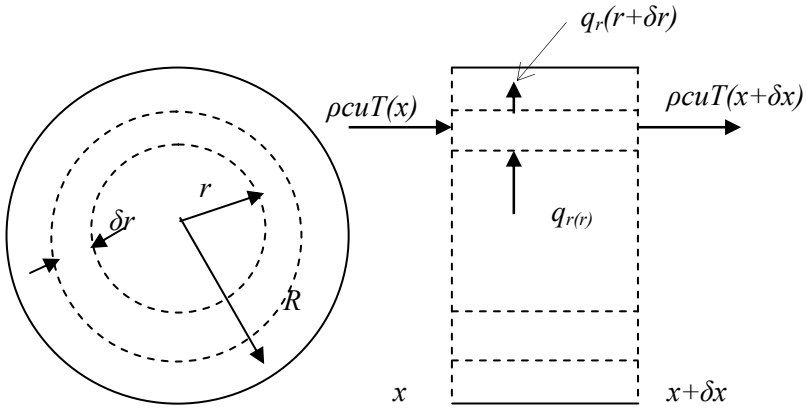

FIGURE 5: Heat balance in a small cylindrical shell in a pipe-flow model (Turcotte and Schubert, 2003).

If the flow is steady, the temperature of the fluid does not change with time and if axial heat conduction is unimportant compared with advection of heat by the flow, the net effects of radial heat conduction and heat advection must balance each other (Turcotte and Schubert, 2003):

$$u\rho c\frac{\partial T}{\partial x}=k\left(\frac{\partial^2 T}{\partial r^2}+\frac{\partial T}{\partial r}\right) \tag{85}$$

The assumption of neglecting viscous dissipation, or frictional heating, is also made. In a laminar case, the velocity as a function of mean velocity $\bar{u}$ is calculated by (Turcotte and Schubert, 2003):

$$u=2\bar{u}\left[1-\left(\frac{r}{R}\right)^2\right] \tag{86}$$

The case in which the wall temperature of the pipe is T_w and the fluid temperature is changing linearly along the length as (Turcotte and Schubert, 2003) gives:

$$T_w=c_1x+c_2;T=c_1x+c_2+\theta(r)=T_w+\theta(r) \tag{87}$$

where c_1 and c_2 are constants; and
$\theta(r)$ is the temperature difference between the fluid and the walls.

By putting this into Equation 85, the following equation is obtained:

$$2\rho c\bar{u}\left[1-\left(\frac{r}{R}\right)^2c_1\right]=k\left(\frac{\partial^2\theta}{\partial r^2}+\frac{1}{r}\frac{\partial\theta}{\partial r}\right) \tag{88}$$

The boundary conditions are: $T=T_w$ at $r=R$ and $q_r=0$ at $r=0$. The latter condition is required because there is no line source or sink along the axis of the pipe. The first condition is satisfied if $\theta_{r=R}=0$ while the second one becomes $(d\theta/dr)_{r=0}=0$, with the aid of Fourier's law. The solution of Equation 88 with these boundary conditions is:

$$\theta = -\frac{\rho c \bar{u} c_1 R^2}{8k}\left(3 - 4\frac{r^2}{R^2} + \frac{r^4}{R^4}\right) \tag{89}$$

Applying Fourier's law at $r = R$, the heat flux through the wall q_w is found to be as follows:

$$q_w = -\frac{1}{2}\rho c \bar{u} R c_1 \tag{90}$$

This flux is constant and independent of x. If c_1 is positive, the wall temperature increases in the direction of the flow, and heat flows through the wall of the pipe into the fluid. If its value is negative, the wall temperature decreases in the direction of flow, and heat flows out of the fluid into the wall of the pipe. The heat flux to the wall can be expressed through the coefficient of heat transfer h between the wall heat flux and the excess fluid temperature according to:

$$q_w = h(\bar{T} - T_w) = h\bar{\theta} \tag{91}$$

The average flow of the excess fluid temperature (for unit area) is calculated by:

$$\bar{\theta} = \frac{2\pi\int_0^R (\theta u r)dr}{\pi R^2 \bar{u}} = -\frac{11\rho c \bar{u} c_1 R^2}{48k} \tag{92}$$

In order to calculate the value of the coefficient h, Equations 90 and 91 are combined:

$$h = \frac{48k}{11D};\ \ D = 2R \tag{93}$$

Equation 93 is valid only for R_e < 2200 (laminar flow). For pipe flow with heat addition, a dimensionless measure of the heat transfer coefficient is introduced, known as the Nusselt number, N_u, which is a measure of the efficiency of the process. This coefficient is calculated by (Turcotte and Schubert, 2003):

$$N_u \equiv \frac{hD}{k} = \frac{48}{11} \approx 4.36 \tag{94}$$

For the above difference in temperatures, fluid film thickness D and conductivity k, the conductive heat flux would be:

$$q_c = \frac{k\left(\bar{T} - T_w\right)}{D} = \frac{q_w k}{Dh} \Rightarrow N_u = \frac{q_w}{q_c} \tag{95}$$

4.4 Aquifer model for hot springs

The model of Figure 6 is considered. If the heat convected along the aquifer is balanced against the heat lost or gained by conduction to the walls, it leads to (Turcotte and Schubert, 2003):

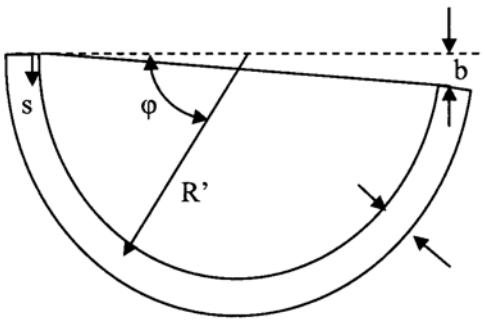

FIGURE 6: Model of a semicircular pipe-like aquifer simulating a hot spring (Turcotte and Schubert, 2003)

$$\pi R^2 \rho c \bar{u} \frac{d\bar{T}}{ds} = 2\pi R h\left(T_w - \bar{T}\right) \tag{96}$$

where s is the distance measured along the aquifer; its relation with the angle is: $s=R'\varphi$.

It is assumed that the wall temperature of the aquifer depends on the local geothermal gradient β as follows:

$$T_w = R'\beta\sin\varphi + T_0 \Rightarrow \frac{R^2\rho c\bar{u}}{R'}\frac{\partial\bar{T}}{\partial\varphi} = \frac{48}{11}k\left(R'\beta\sin\varphi + T_0 - \bar{T}\right) \tag{97}$$

Equation 97 can be simplified through the introduction of the Pèclet number ($P_e = \rho c\bar{u}R/k$) and the Prandtl number ($P_r = \rho cv/k$) and finally the introduction of the dimensionless temperature as follows (Turcotte and Schubert, 2003):

$$\frac{11}{48}\frac{R}{R'}P_e\frac{\partial\theta}{\partial\varphi} + \theta = \sin\varphi \tag{98}$$

The solution of this linear first order differential equation with appropriate boundary conditions is:

$$\bar{T} = T_0 \ or \ \theta = 0 \ at \ \varphi = 0$$

$$\theta = \left[\frac{48R'}{11RP_e}\sin\varphi - \cos\varphi + \exp\left(-\frac{48}{11}\frac{R'}{RP_e}\varphi\right) * \left(\frac{48}{11}\frac{R'}{RP_e}\right)\right] * \left(\frac{48}{11}\frac{R'}{RP_e}\right)\left[1 + \left(\frac{48}{11}\frac{R'}{RP_e}\right)\right]^{-1} \tag{99}$$

The dimensionless temperature θ_e at the exit of the aquifer, at $\varphi=\pi$, is given by (Turcotte and Schubert, 2003):

$$\theta_e = \frac{\left[\exp\left(-\frac{48}{11}\frac{R'\pi}{RP_e}\right)+1\right]\frac{48}{11}\frac{R'}{RP_e}}{1+\left(\frac{48}{11}\frac{R'}{RP_e}\right)^2} \tag{100}$$

4.5 One dimensional advection of heat in a porous medium

It is well known that geothermal systems develop above magma bodies, hot intrusions and hot crustal regions, which induce large scale motions of groundwater in the rocks above. A substantial fraction of hot springs with exit temperatures of about 50°C is believed to be the direct result of this type of hydrothermal circulation. The heat source heats the groundwater, which becomes less dense and rises. Near the Earth's surface the water cools and becomes denser. It can then sink and recharge the aquifers and porous rock in the vicinity of the heat source. The water is then reheated, and the cycle repeats. An analysis of the complete hydrothermal convection system requires the solution of a coupled set of nonlinear differential equations in at least 2-D.

Here the upwelling flow above the heat source is studied. An incompressible fluid flows through the rock-matrix (porous medium) with velocity components u (x-direction) and v (y-direction). In this case (Turcotte and Schubert, 2003):

$$\frac{\partial u}{\partial x} + \frac{\partial v}{\partial y} = 0 \tag{101}$$

The energy conservation equation can be written (Turcotte and Schubert, 2003):

$$\rho_m c_{p_m} \frac{\partial T}{\partial t} + \rho_f c_{p_f} \left(u \frac{\partial T}{\partial x} + v \frac{\partial T}{\partial y} \right) = \lambda_m \left(\frac{\partial^2 T}{\partial x^2} + \frac{\partial^2 T}{\partial y^2} \right) \tag{102}$$

For steady 1-D flow (dv/dy=0) Equation 102 can be simplified as follows (Turcotte and Schubert 2003):

$$\rho_f c_{p_f} \left(v \frac{\partial T}{\partial y} \right) = \lambda_m \left(\frac{\partial^2 T}{\partial y^2} \right) \tag{103}$$

Integration of Equation 103 gives:

$$\rho_f c_{p_f} vt = \lambda_m \frac{\partial T}{\partial y} + c_1 \tag{104}$$

The value of the integration constant c_1 can be determined from the conditions at great depth where upwelling fluid has the uniform reservoir temperature T_r. Therefore $y \rightarrow \infty$ leads to ($dT/dy \rightarrow 0$ and $T \rightarrow T_r$). This gives $c_1 = \rho_f c_{pf} v T_r$, and (Turcotte and Schubert, 2003):

$$\rho_f c_{p_f} v(T - T_r) = \lambda_m \frac{\partial (T - T_r)}{\partial y} \tag{105}$$

This equation is rearranged as follows:

$$\frac{d(T - T_r)}{(T - T_r)} = \frac{\rho_f c_{p_f} v}{\lambda_m} dy \tag{106}$$

The integration of Equation 106 gives:

$$\ln \frac{(T - T_r)}{c_2} = \frac{\rho_f c_{p_f} v}{\lambda_m} y \;\; or \;\; (T - T_r) = c_2 \exp\left(\frac{\rho_f c_{p_f} v}{\lambda_m} y\right) \tag{107}$$

As ($y \rightarrow \infty$) the right side of Equation 107 approaches zero, because $v < 0$. In order to evaluate the integration constant c_2, T is set to T_0 at the surface (y=0) and then $c_2 = T_0 - T_r$ and also:

$$T = T_r - (T_r - T_0) \exp\left(\frac{\rho_f c_{p_f} v}{\lambda_m} y\right) \tag{108}$$

If the flow is driven by the buoyancy of the hot water, the Darcy velocity can be used to estimate the permeability of the system. Darcy's law can be written as:

$$v = -\frac{k}{\mu} \left(\frac{dp}{dy} - \rho g \right) \tag{109}$$

Buoyancy forces are caused by a decrease in density (because of heating), described by (Turcotte and Schubert, 2003) as:

$$\rho_f = \rho_{f0} - \alpha_f \rho_{f0} (T_r - T_0) \tag{110}$$

where ρ_{f0} = Water density at T_0
α_f = The coefficient of thermal expansion

Inserting Equation 110 into Equation 109 gives:

$$v = -\frac{k}{\mu} \left(\frac{dp}{dy} - \rho_{f0} g \right) - \frac{k}{\mu} \alpha_f \rho_{f0} g (T_r - T_0) \tag{111}$$

By making the assumption that $dp/dy \approx 0$, Equation 111 can finally be written as (Turcotte and Schubert, 2003):

$$v = -\frac{k}{\mu}\alpha_f \rho_{f0} g\left(T_r - T_0\right) \tag{112}$$

5. DISTRICT HEATING SYSTEM USING THE GEOTHERMAL WATER

In general, geothermal water for a district heating system is taken directly from low-temperature reservoirs. Another way is to run the geothermal water through heat exchangers to heat up fresh water. The hot water can be stored in tanks if appropriate. This water is then transmitted to buildings and can be used for heating and tap water. Heat flow to the buildings is controlled by the mass flow. A sketch of a geothermal district heating system is given in Figure 7.

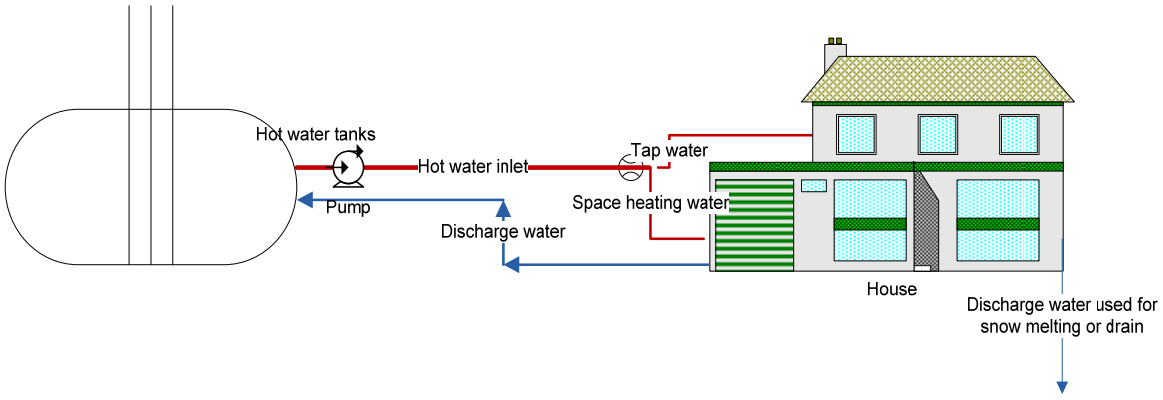

FIGURE 7: A sketch showing the main elements of a geothermal district heating system

In the following the basic calculations for geothermal district heating are presented. The main elements of geothermal district heating are radiators. Such a system is affected by the water's thermal energy, building heat loss, pipe heat loss and building energy storage. A short description for each of them is given below.

5.1 Radiators

Radiators are heat exchangers that make it possible to transfer heat from geothermal water to the indoors surroundings. The relative heat capacity of a radiator is given by the following relationship:

$$\frac{Q^{rad}}{Q_0^{rad}} = \left(\frac{\Delta T_m}{\Delta T_{m0}}\right)^{4/3} \tag{113}$$

where the subscript 0 denotes design conditions.

The temperature difference ΔT_m is calculated (Nappa, 2000) by:

$$\Delta T_m = \frac{\left(T_s - T_i\right) - \left(T_r - T_i\right)}{\ln\left(\frac{T_s - T_i}{T_r - T_i}\right)} = \frac{T_s - T_r}{\ln\left(\frac{T_s - T_i}{T_r - T_i}\right)} \tag{114}$$

5.2 Thermal energy of the water

The water's thermal energy which is transferred to the indoor surroundings through the radiators is:

$$Q^{rad} = c_p m\left(T_s - T_r\right) \tag{115}$$

where subscripts *s* and *r* denote supply and return, respectively.

The relative thermal energy given by the geothermal water is (Nappa, 2000):

$$\frac{Q^{rad}}{Q_0^{rad}} = \frac{m\left(T_s - T_r\right)}{m_0\left(T_{s0} - T_{r0}\right)} \tag{116}$$

5.3 The building heat loss

The biggest energy loss in a geothermal district heating system may come from the buildings. These losses can be calculated as (Nappa, 2000):

$$Q_{loss} = k_l\left(T_i - T_0\right) \tag{117}$$

where the building heat loss factor k_l is assumed constant.

The relative losses are (Nappa, 2000):

$$\frac{Q_{loss}}{Q_{los0}} = \frac{T_i - T_0}{T_{i0} - T_{o0}} \tag{118}$$

5.4. Pipe heat loss

Other heat losses in such system are through the pipes. To determine the amount of loss in the pipes, it is necessary to know the pipe transmission effectiveness parameter τ. Its value (Valdimarsson, 1993) is given by:

$$\tau = \frac{T_s - T_g}{T_1 - T_g} = e^{-\frac{U_p}{mc_p}} \tag{119}$$

The reference value τ can be calculated from the reference flow conditions as follows:

$$\tau_0 = \frac{T_{s0} - T_g}{T_{10} - T_g} = e^{-\frac{U_p}{m_0 c_p}} \tag{120}$$

The values of U_p and c_p are assumed to be constant in the system. By combining Equations 119 and 120, the transmission effectiveness can be calculated:

$$\tau = \tau_0^{\frac{m_0}{m}} \tag{121}$$

The supply temperature to the house can be calculated as:

$$T_s = T_g + \left(T_1 - T_g\right)\tau = T_g + \left(T_1 - T_g\right)\tau_0^{\frac{m_0}{m}} \tag{122}$$

and the return water temperature at the pumping station is calculated as:

$$T_2 = T_g + (T_r - T_g)\tau = T_g + (T_r - T_g)\tau_0 \frac{m_0}{m} \tag{123}$$

5.5 Building heat storage

A building's heat storage (dependent on the amount of thermo-insulation) can be very helpful for the heating system. Normally the buildings are like heat storage. A building's heat storage is calculated by (Nappa, 2000):

$$\frac{dT_i}{dt} = \frac{1}{C} Q_{net} = \frac{1}{C}\left(Q_{\sup} - Q_{loss}\right) = \frac{1}{C}\left[mc_p(T_s - T_r) - k_l(T_i - T_0)\right] \tag{124}$$

where C is the total heat capacity of the building.

5.6 Pipe and distribution network design

The network's design is affected by a number of factors, the most important of which are: topology and route selection, pump station design, and pipe system, tanks and pressure vessels (structural design). After all the necessary calculations are made, a cost evaluation process must be done, in order to optimise the design.

5.7 Pipe design

The pipe design is maybe the most important part of the network system and, at the same time, the most costly. The standard design process for the pipelines is:

- Topology and route selection;
- Demand and flow analysis;
- Pipe diameter optimisation;
- Thickness and pressure classes;
- Mechanical stress analysis (support, type and distance between them);
- Thermal stress analysis (expansion loops, expansion units);
- Pump size and arrangement.

All these calculations are done with the purpose of minimising the total cost (to optimise the calculations and selections).

5.8 Route selection

The route selection is the first step of these calculations, including the process of identifying constraints, avoiding undesirable areas, etc. In that phase, many factors are evaluated such as the integrity of the pipeline, environmental impacts, public safety, land-use efficiency, proximity from existing facilities, length of the path (attempting to select the shortest) and slopes. There are many ways to make this selection, including cost modelling comparison or transformation of the variable topography distance.

5.9 Pipe diameter and wall thickness

Deciding on the pipe diameter is another important step in the calculations. Here, the maximum allowable velocity and of course the minimisation of the total cost (updated) are taken into account. Pressure is one of the most important design criteria. The design pressure value should be higher than the pressure under the most severe conditions. The pressure is calculated by taking into account the friction losses (Jónsson, 2007):

$$H_f = f\frac{v_{hw}^{\ 2}}{2}\frac{L_{pipe}}{d_i} \tag{125}$$

The friction factor depends on the flowing regime and can be calculated:

$$f = \frac{64}{R_e} \quad for \quad R_e < 2100 \ (laminar\ flow)$$

$$\begin{cases} f = \dfrac{0.361}{(R_e)^{\frac{1}{4}}} \\ \dfrac{1}{\sqrt{f}} = 1.14 - 2\log\left(\dfrac{k}{d_i} + \dfrac{9.35}{R_e\sqrt{f}}\right) \end{cases} \quad for\ R_e > 2100 \ (turbulent\ flow) \tag{126}$$

Now it is possible to calculate the pressure for the pump and the power of the motor through the relationship:

$$P_{pump} = P_c + P_h + \frac{H_f \rho_w g}{10^5}; \quad P_m = \frac{Q_w P_{pump}}{\eta_p \eta_m} \tag{127}$$

When all prices are known, including electricity, pipes, junctions, bends, valves and pump it is possible to calculate the costs (operative and capital costs). The design process continues with calculations of thickness. The thickness based on the pumping pressure can be calculated as (Jónsson, 2007):

$$\delta = \frac{P_{pump} d_o}{2\left(S_a + P_{pump} y\right)} + \delta_a \tag{128}$$

5.10 Thermal stress analysis

The geothermal water pipeline is working under conditions of elevated values of pressure and temperature. Because of the elevated temperature, the pipe is constrained and this movement should be controlled. This control is realised between the expansion loops, expansion units or by using pre-stressed pipes. The thermal expansion, the stress and the force are calculated as follows:

$$\Delta L = \alpha L_{pipe} \Delta T; \ \ \sigma = E\frac{\Delta L}{L_{pipe}}; \ \ F = \pi\frac{d_i^2}{4} E\alpha\Delta T \tag{129}$$

And finally the expansion arms as (Jónsson, 2007):

$$L_a = \frac{\sqrt{d_o \alpha \Delta T L_{anchor}}}{208.3\left(2-\sqrt{2}\right)^2} \tag{130}$$

5.11 The pressure vessels

During the design phase of the pressure vessels, there are several constraints such as: classification, diameter and thickness, form, supports (type), saddle (size) and openings (reinforcement). The classification of the pressure vessels is made on the basis of the maximum allowable pressure, their volume and the stored fluid. The thickness is calculated again for the most severe conditions of differential pressure and temperature. The first step in the calculation procedure for the tank consists of its optimisation (minimising the area). The function to be minimised is (Jónsson, 2007):

$$A = \pi DH + 2\pi \frac{D^2}{4} \tag{131}$$

The minimum is obtained by $D = |H|$.

The plate and roof thickness can be calculated by:

$$\delta_p = \frac{P_t D_{\min}}{2 f_{\tan k} W_{factor}^{\tan k}} + \delta_{ad}^{\tan k}; \quad \delta_r = \frac{40 D_{\min}}{2 \sin \Theta \sqrt{20 P_{atm} \dfrac{100}{E_y}}} \tag{132}$$

6. RESULTS OF SIMPLE HOT SPRING MODELLING

The six hot water springs at Llixha in the Elbasan region have water temperatures up to 65°C and a flow-rate up to 23 l/s. Estimated reservoir temperature at depth associated with the hot springs, based on the chemical composition using different geothermometers, is given in Table 2.

TABLE 2: Estimated water temperature (°C) at depth based on different geothermometers (Frashëri et al., 2004)

Geothermometer	Spring "Nosi" Llixha, Elbasan
Fournier	254
Truesdell	235
Na+Ka+Ca	143

These values indicate that the water is coming from a great depth where the average temperature is over 200°C. The mineralisation of the water is 7.2 g/l, the H_2S content 410 mg/l and free CO_2 180 mg/l. The high content of CO_2 makes the Na+Ka+Ca geothermometer unreliable so the reservoir temperature is likely to be in the range of 220-235°C (Arnórsson, 2000; 2007; Arnórsson and D'Amore, 2005). This is in agreement with calculations based on the geothermal gradient and a depth of 4500-5000 m. Its value for the region is of the order of 30°C/km as is shown in Figure 8 (Frashëri et al., 2004).

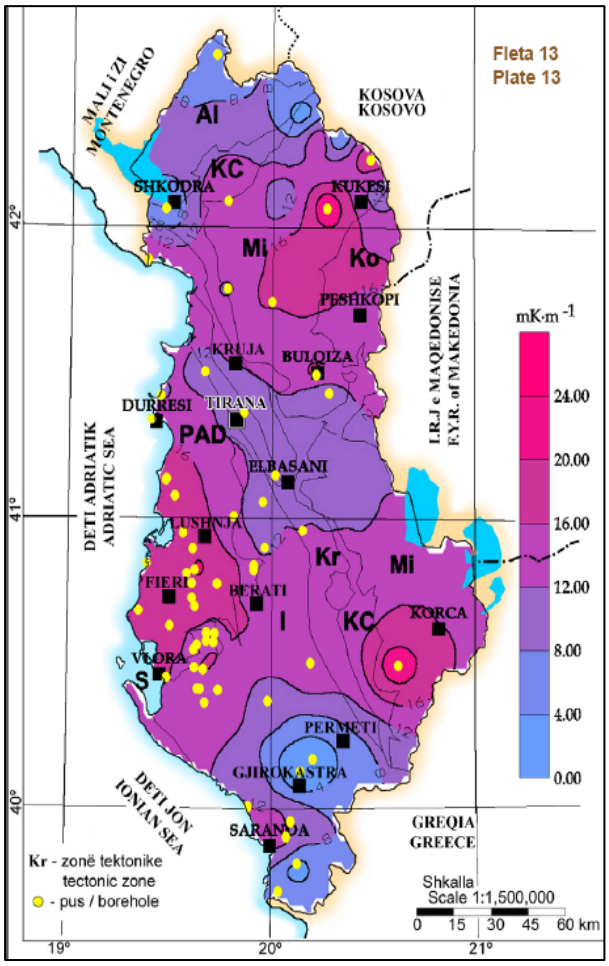

FIGURE 8: Temperature gradient map of Albania

The water contains < 1.2% tritium. The absence of tritium shows that it originated as precipitation centuries ago. The waters are chloro-magnesial and contain the cations Ca^{+}, Mg^{+} and Na^{+} and the anions Cl^{-}, SO^{4-} and HCO^{3-}. The Ph is in the range 6.8-7 and the density 1000-1060 kg/m^3. As shown in Figure 9 (Frashëri et al., 2004), the hot springs are situated in the middle of the village. The hot water has only been used for balneology, but this has been done for many centuries, possibly since the time of the Roman Empire. The first modern use dates back to 1937 with the building of the "Hotel Park" medical centre. The use of the water flowing from these springs can help to improve the economical effectiveness of district heating in the village. The realisation of such a project will allow the utilization of geothermal water as an energy resource for the first time in Albania. The purpose of the calculations presented in this chapter is to show that the water from these hot springs can be used for district heating of the village community.

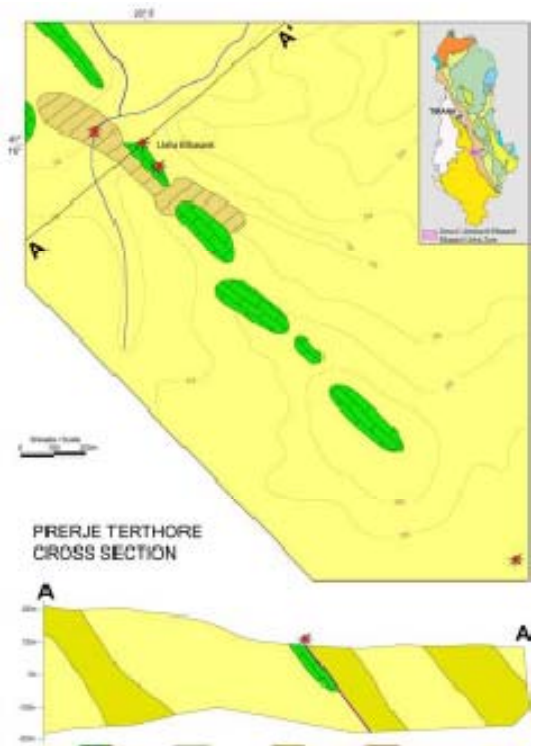

FIGURE 9: Geomorphological map of the Llixha region

6.1 The 3-D modelling of the temperature field of Llixha, Elbasan region

A finite volume model was set up for a crustal volume with an area of 10 × 10 km and 5 km thickness to model the temperature, density and fluid velocity distribution in the Llixha region. The grid is shown in Figure 10. Here, it is assumed that the medium is homogeneous and isotropic and that $k_x = k_y = k_z = 2$ W/m°K (Osmani, 1987). It is also known that Q = 20 l/s (corresponding to $m_i = Q/6 = 3.3$ l/s or 3.224 kg/s for each of the hot springs), c_p =4180 J/kg°C. The temperature at depth in the formation is set at 221°C while the temperature of the water at the surface is in the range 60-65°C. The temperature gradient of the surroundings is assumed to be 12°C/km (see Figure 8).

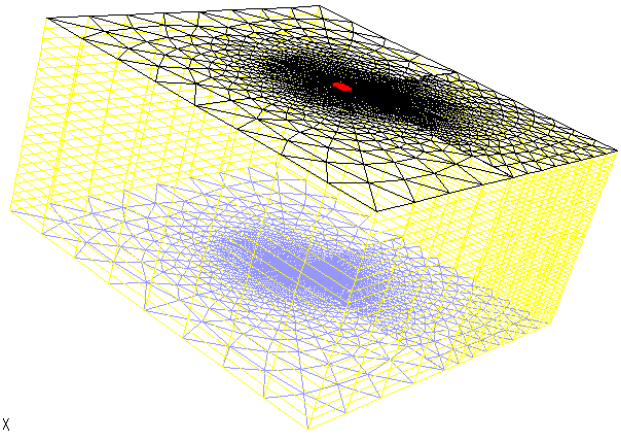

FIGURE 10: The finite volume grid used to model temperature and flow conditions in the Llixha region

The modelling software FLUENT is used to solve the problem, providing calculated results for temperature, density and velocity for the volume modelled. In the model, water flows with a velocity of 1.25×10^{-7} m/s. The results for temperature, density and velocity, as well as velocity vectors, are shown in Figures 11, 12, 13 and 14. More details on the modelling using FLUENT are presented in Appendix I.

In conclusion, we can say that the results of finite element calculations (Section 4 and Appendix I) and the FLUENT modelling can help predicting the future temperature changes on the ground if the flow from the hot springs should change.

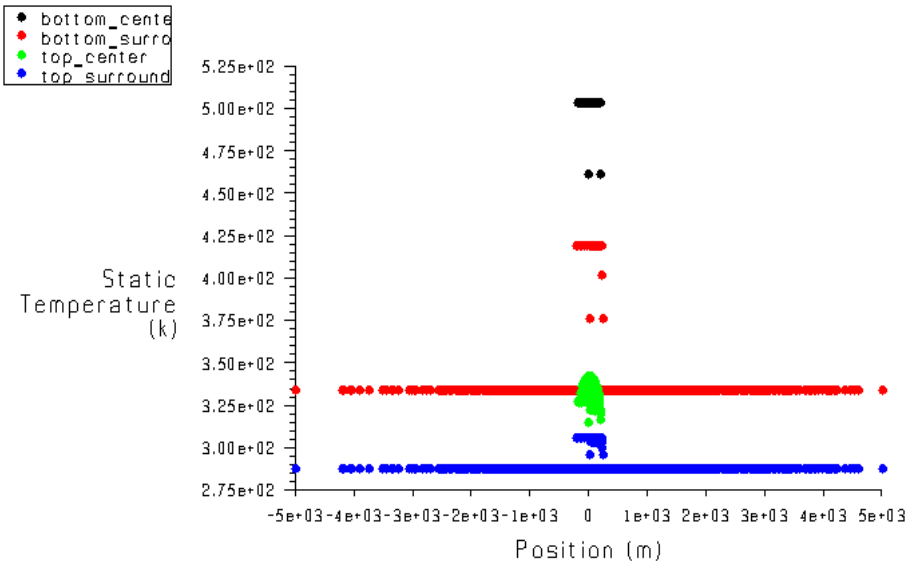

FIGURE 11: The temperature magnitude

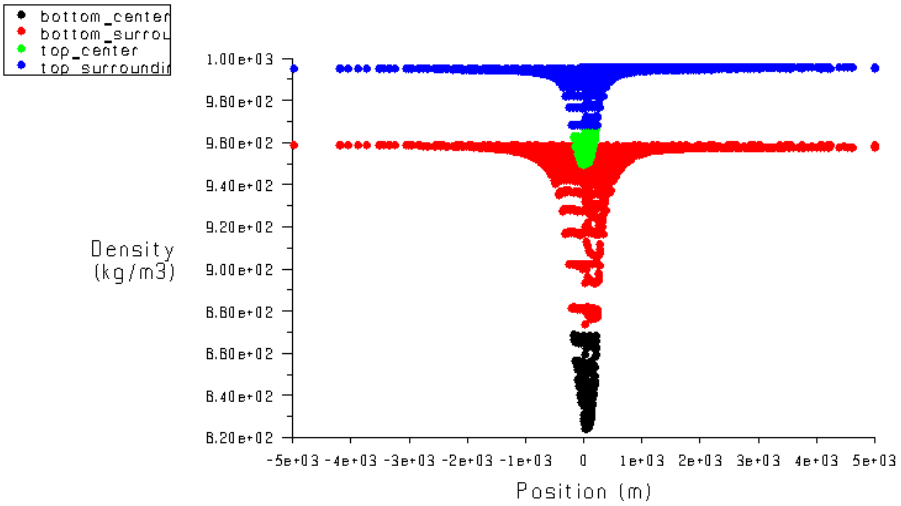

FIGURE 12: The density magnitude

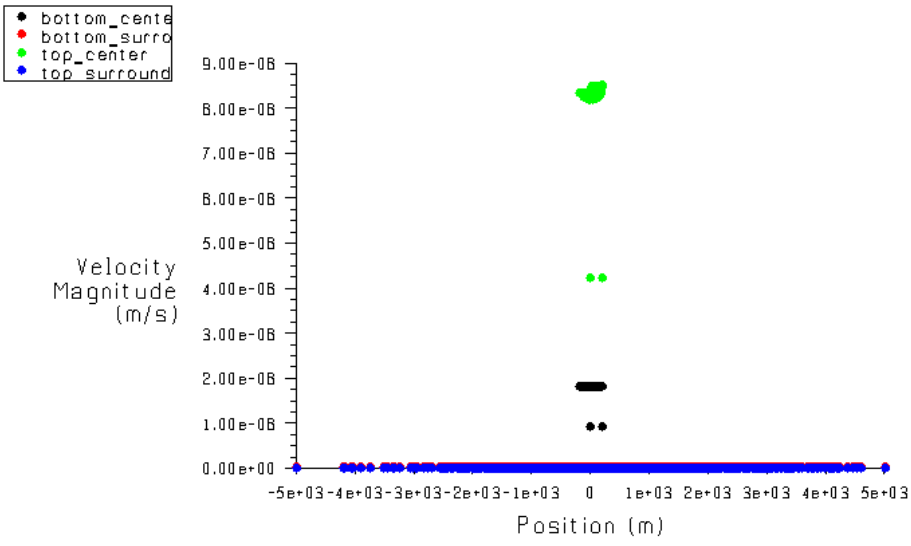

FIGURE 13: The velocity magnitude

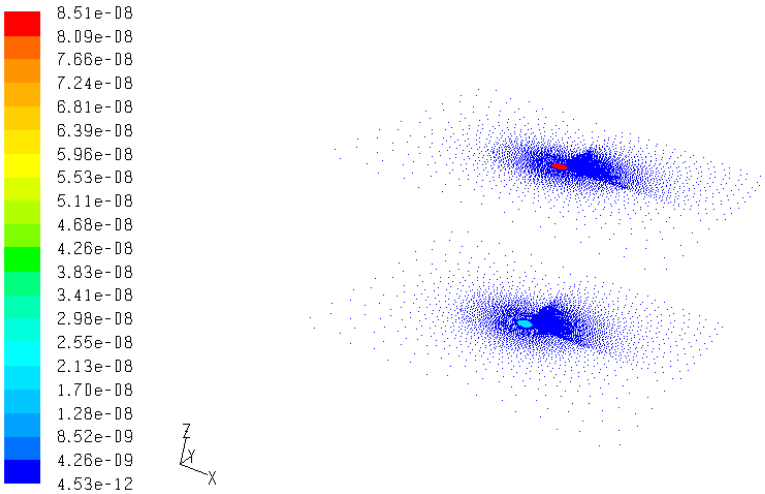

FIGURE 14: The velocity vectors

6.2 Calculation results for the hot spring dynamics

The purpose of these calculations is to estimate the water temperature in the formation, to estimate formation properties and to find how the temperature changes in the upflow zone of the spring water. The water table was assumed to move at a velocity of 4 m/year. The temperature of the rocks is assumed to be about 230°C, the radius R' = 14.4 m, the geothermal gradient β = 30°C/km, the inflow 20 l/s, the value of the angle $\varphi = \pi/6$, the thermal diffusivity $\kappa = 1.4\times10^{-7}$ m^2s^{-1} and the convection coefficient heat transfer α= 3×10^{-5} K^{-1} (Turcotte and Schubert, 2003).

Solving the problem, shows the water temperature in the reservoir estimated at about 221°C (quite similar as indicated by the geothermometers), the permeability of the formation is about 8.8 mD, the drainage area of the formation is about 0.1575 km^2 and the temperature of the upflowing water changes as shown in Figure 15.

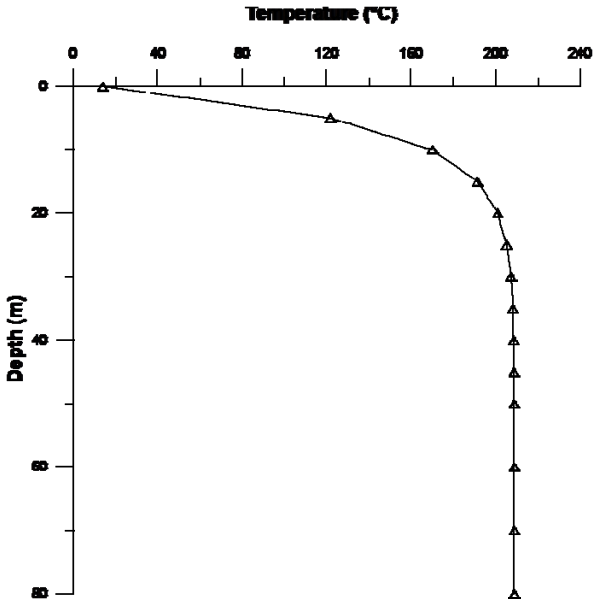

FIGURE 15: The temperature change with the upflow of the water

7. BASIC DISTRICT HEATING DESIGN

7.1 Results for the network system

The pipeline was assumed to be composed of two parts: part one being 2 km in length and part two being 3 km in length. The flow baseline was assumed to be 20 l/s and the temperature of the water 65°C, the pressure at consumption should be 2.31 bar.

Calculations were made for 4 different diameters in the range 0.07-0.111 m. The basic restriction was the water flow velocity. If this value is greater than 3-4 m/s, noises level, corrosion and erosion ratios

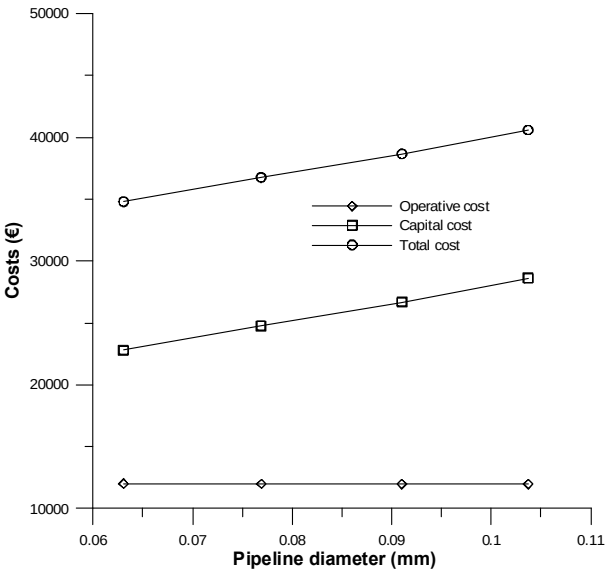

FIGURE 16: Pipeline optimisation

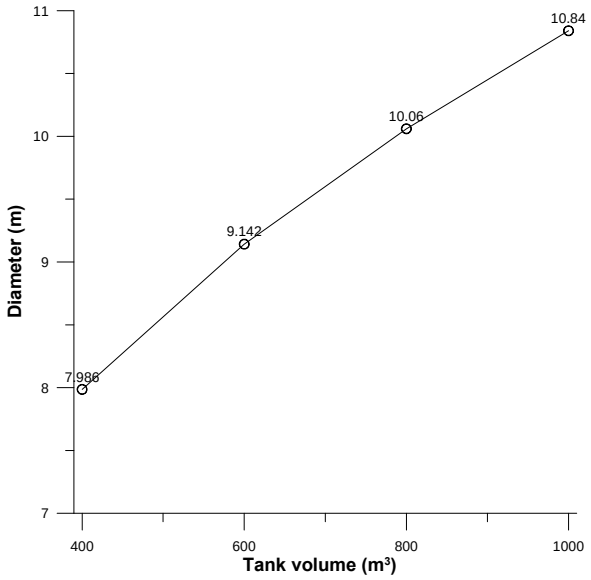

Figure 17: Tank area optimisation

are too high. Under these conditions, pipeline optimisation, based on the total cost, shows that the optimal diameter is 0.090 m (see Figure 16). The calculations for the tank are made for four different volumes in the range of 400-1000 m^3. The surface optimisation of the tank shows that the optimal diameter is in the range of 8.0-10.8 m (Figure 17). The numerical results of the calculations are presented in Appendix II.

7.2 Calculation for the radiators

The steps used to calculate the radiator parameters are given in Sections 5.1-5.5. In these calculations, it was assumed that the supply temperature of the water is 60°C, the reference temperature 65°C, and the ground temperature 6°C. The calculations were done for 4 different scenarios: The indoor temperature was assumed to be in the range 18-20°C, the outdoor temperature in the range -10 to -4°C, the return water temperature in the range 33-40°C, the reference inflow in the range of 3.9-7 kg/s, and the reference system inflow 18-24 kg/s. Based on these data, the relative heating of the radiators was calculated as 0.83-0.92, the relative heating of the building as 0.87-0.88, and the transmissivity coefficient as $\tau = 0.94$. To be within these parameters, it is sufficient that the supply water temperature be 60°C, and the inflow of the system 16-27 kg/s. The parameters for the Llixha thermal springs satisfy all these demands. Figure 18 shows the results of calculations for the radiators supply and return water temperatures vs. indoor temperature. The relevant calculations are done with EES (Engineering Equation Solver) and the results given in Appendix III.

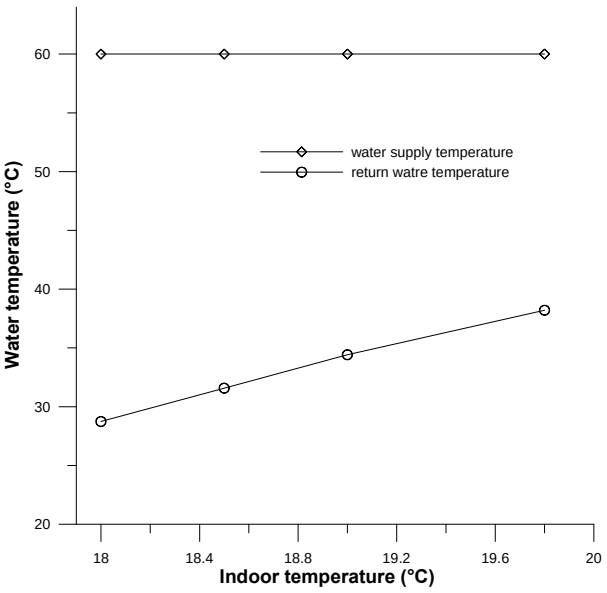

FIGURE 18: Calculations for the radiators

8. CONCLUSIONS

Based on calculations presented in this report the following can be concluded regarding utilization of the hot springs of the Llixha-Elbasan hot-spring area in Albania:

- The water temperature is expected to be stable in the future;
- The geothermal reservoir temperature at 4500-5000 m depth is thought to be about 220°C;
- The water starts to cool down when it reaches 160 m depth;
- The geothermal water from the Llixha hot springs fulfils all requirements for district heating in the region;
- Considerably higher water temperature is expected through further well drilling.

ACKNOWLEDGEMENTS

I would like to express my gratitude to the United Nations University and to the Government of Iceland for giving me the chance to participate in the Geothermal Training Programme in Iceland. I would also like to express my thanks to Dr. Ingvar B. Fridleifsson and Mr. Lúdvík S. Georgsson for all their help in each step of my training program. My most sincere thanks go to my supervisors, Gudni Axelsson and Halldór Pálsson, for their help and their advice in completing the report. Finally, and last but not least, I express my best wishes and thanks to the wonderful staff of the UNU-GTP for their help and support.

My wishes and thanks also go to all the UNU-GTP Fellows in 2007!

NOMENCLATURE

A_o = T-change amplitude of the ground
b_i = Fractures' mean width [m]
C = Heat capacity of the house [J/kg K]
C_t = Total compression of the system
C_u = Isobaric capacity of specific heat of the water
c = Constant which takes into account the properties of the fluid and the rock
c_p = Fluid specific heat [J/kg K]
D = Effective thickness
D_i = Fractures' mean diameter
DH_o = Radioactive heat on the upper part of the earth's crust
d_i = Inner diameter of the pipeline
d_o = Outer diameter of the pipeline
f = Volume of incondensable gas (gaseous phase)
f_f = Friction factor
H_o = Constant
H_f = Friction losses
k_v = Permeability [m^2]
k_x, k_y, k_z = Thermal conductivity in ox, oy, oz [W/m K]
L = Amount of energy for unit of mass
L_{anchor} = Anchor length

L_{pipe} = Length of the pipeline
L_{wv} = Heat needed for water evaporation
M = Isobaric volume heat capacity for the phases (ro rock , o oil, w water, g gas)
M_R = Effective volume capacity
m = Mass of particles [g]
m = Water mass flow [kg/s]
m_0 = Reference water mass flow
N = Number of fractures
I = Installation cost for a single well
$I_{\$}$ = Maintenance cost for a single well
P = Price
P_c = Pressure at the consumer
P_d = Periods
P_h = Hydrostatic pressure
p = Pressure [Pa]
$Q=Q(x, y, z)$ = Volume density of the source
Q^{rad} = Heat capacity of the hot water
Q_0^{rad} = Heat capacity of the hot water at the reference conditions
Q_{loss} = Heat losses [W]
Q_{loss0} = Heat losses at the reference conditions
Q_{net} = Net heat
Q_w = Flowrate [m^3/s]
q_o = Heat flow density (=c^{te})
q_r = Radioactive heat on the upper mantle
R = Drainage radius of the well
Re = Reynolds number
R_o = Exertion coefficient for the reinjection well
r = Well radius
S = Saturation of the formation
S_a = Allowable stress [Pa]
t = Time
$T=T(x, y, z)$ = Temperature
T_o = Ground extrapolated temperature
T_o^a = Air temperature in a given time
T_f , T_d = Transitory temperatures (frost, dried)
T_g = Ground temperature
T_i = Initial temperature
T_i = Indoor temperature
T_r = Reinjection water temperature
T_r = Return water temperature
T_{r0} = Reference return water temperature
T_s = Water supply temperature (primary network)
T_{s0} = Reference water supply
U_p = Pipe heat loss factor
v = Velocity of particles [m/s]
w = Ice amount for the dried zones
y = Resultant movement

Greek letters

α = Coefficient of thermal expansion
β = Coefficient which takes into account the formation composition (Btu/lb°F)
δ = Pressure coefficient of the thermal conductivity
Δt = Duration of the installations
ε = Surface radiation coefficient

ω = Angular frequency
Φ = Porosity
Θ = Angle of the tanks roof
λ_o = Conductivity in normal pressure
λ_c = Thermal convection coefficient [W/m^2 K]
λ_e = Thermal diffusion coefficient
γ_c = Effect of heat convection in its transfer
λ_f , λ_d = Thermal conductivity (frost, dried) [W/m K]
λ_i = Thermal conductivity on the deep ΔZ_i
μ = Viscosity (dynamic) [kg/m s]
η_m = Motor efficiency
η_p = Pump efficiency
$\rho_{(ro,\ o,\ w,\ g)}$ = Density of the (rock, oil, water, gas) [kg/m^3]
ρ_m = Average density
ρ_v = Vapour density
ρ_w = Water density
τ_0 = Pipe transmission effectiveness at reference conditions

REFERENCES

Aliaj, S., and Hyseni, A., 1996: *The neotectonic map of Albania, scale 1:200,000.* Sh.B.L.U., Tirana, 87 pp.

Arnórsson, S., 2000: Mineral saturation. In: Arnórsson, S. (ed.), *Isotopic and chemical techniques in geothermal exploration, development and use. Sampling methods, data handling, interpretation*. International Atomic Energy Agency, Vienna, 241 266.

Arnórsson, S., 2007: *Reactive and conservative components.* UNUGTP, Iceland, unpublished lectures.

Birch, F., and Clark, 1940: The thermal conductivity of rocks and its dependence upon temperature and composition, Part I. *Am. J. of Science, 238*, 529-558.

Carslaw, H.W., and Jaeger, J.C., 1959: *Conduction of heat in solids* (2nd edition). Clarendon Press, Oxford, 510 pp.

Čermák, V. and Haenel, R., 1988. Geothermal maps. In: Haenel, R., Rybach, R. and Stegena, L. (eds.), *Handbook of terrestrial heat flow density determination.* Kluwer Academic Publishers. Dordrecht, Boston and London, 261300.

Frasheri, A., Cermak, V., Doracaj, M., Lico, R., Safanda, J., Bakalli, F., Kresl, M., Kapedani, N., Stulc, P., Malasi, E., Çanga, B., Vokopola, E., Halimi, H., Kucerova, L., and Jareci, E., 2004: *Atlas of geothermal resources in Albania.* Faculty of Geology and Mining, Polytechnic University of Tirana, Tirana.

Hyseni, A., and Kapllani, L., 1995: *Geotectonics of Durrësi region in the outlook of complex geologygeophysical study.* Proceedings of the E.E.G.S. meeting, Torino.

Hyseni, A., and Melo, V., 2000: *The geodynamics of new movements in Albania and their influence on resources and environment.* National Programmes for Research Development, Toena, Tirana.

Jónsson, M.Th., 2007: *Mechanical design of geothermal power plants.* UNUGTP, Iceland, unpublished lectures.

Koçiaj, S., 1989: On the construction of the earth crust in Albania according to the first onset of "P" waves in a seismologic station. *Bull. of Geol. Sciences, 1,* 400410.

Nappa, M., 2000: *District heating modelling*. University of Iceland, report, 47 pp.

Osmani, S., 1987: *Finite elements, applications I.* Sh.B.L.U., Tirana, 210 pp.

Osmani, S., 1997: *Numerical methods.* Sh.B.L.U., Tirana, 125 pp.

Plummer, C.C., and McGeary, D.F.R., 1988: *Physical geology (*4th ed.). Wm.C. Brown Co. Publishers, 535 pp.

Shallo, M., and Daja, S., 2000: *Geodynamics.* Sh.B.L.U., Tiranë, 215 pp.

Turcotte, D., and Schubert, G., 2003: *Geodynamics* (2nd ed.). Cambridge, 580 pp.

Valdimarsson, P., 1993: *Modelling of geothermal district heating systems.* University of Iceland, Ph.D. thesis, 315 pp.

Wu, Y.S., and Pruess, K., 1990: An analytical solution for wellbore heat transmission in layered formations. *SPE Reservoir Engineering, 531538.*

APPENDIX I: Modelling of the Llixha Elbasan reservoir

Equation 74 in Section 4.2 is solved for the volumes shown in Figure 1. In the figure, each node represents one of the hot springs. For each of them we have all the data about coordinates and temperature as given in Table 1.

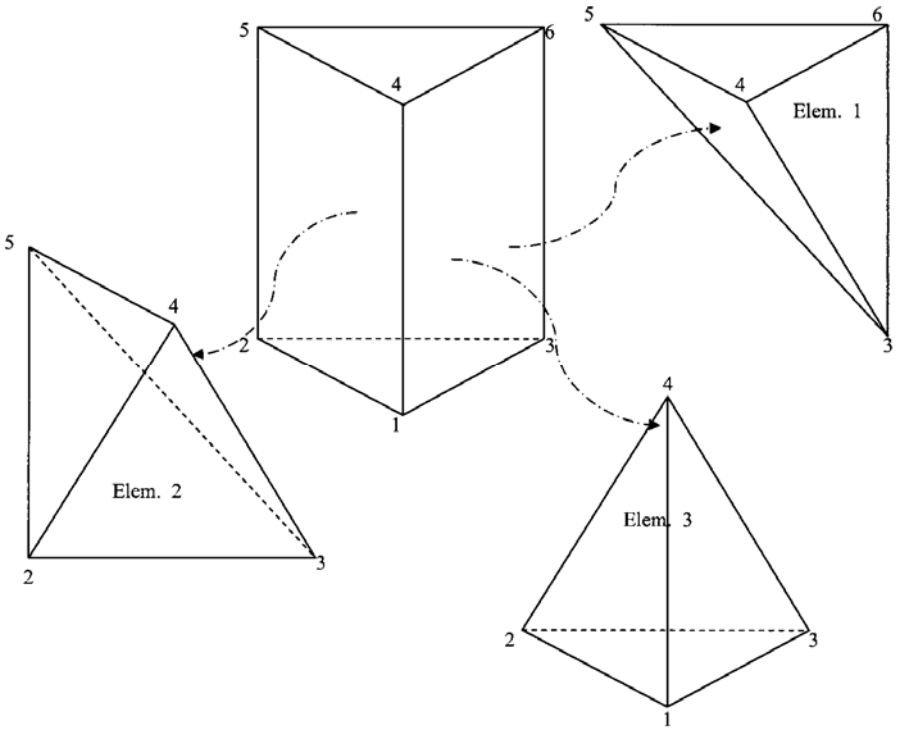

FIGURE 1: The finite volumes

TABLE 1: The coordinates and
the temperatures of the hot springs

Spring (node)	***X* (m)**	***Y* (m)**	***Z* (m)**	***T* (°C)**
1 (1)	0	0	0	60
2 (3)	4	0	0.2	61
3 (2)	4	2	0.3	62.5
4 (4)	8	3	0.25	62
5 (5)	10	5	0.35	63
6 (6)	11	6	0.5	62

Using the relationships given below, the value of the coefficient can be found and the value Δ for each volume. These values are given in Table 2.

TABLE 2: The values of the coefficients

Element 1																
a_1	a_2	a_3	a_4	b_1	b_2	b_3	b_4	c_1	c_2	c_3	c_4	d_1	d_2	d_3	d_4	Δ_1
3.2	0.8	5	10	0.8	0.4	0.5	0.05	2.2	1.15	0.9	0	6	9	3	0	21.1
Element 2																
a_1	a_2	a_3	a_4	b_1	b_2	b_3	b_4	c_1	c_2	c_3	c_4	d_1	d_2	d_3	d_4	Δ_2
5.85	1.2	3.2	2.4	0.25	0.15	0.2	0.2	0.5	0.1	1.4	0	6	2	12	8	5
Element 3																
a_1	a_2	a_3	a_4	b_1	b_2	b_3	b_4	c_1	c_2	c_3	c_4	d_1	d_2	d_3	d_4	Δ_3
0	0	0	2.4	0.4	0.6	0.3	0.2	0.4	0.6	1.3	0.4	8	12	4	8	4.8

The coefficients can be calculated using the following relationships:

$$
\begin{cases}
a_1 = x_2y_3z_4 + x_4y_2z_3 + x_3y_4z_3 - x_4y_3z_2 - x_2y_4z_3 - x_3y_2z_4 \\
a_2 = z_1y_3x_4 + x_3y_1z_4 + x_1z_3y_4 - x_1y_3z_4 - y_1x_3z_4 - z_1x_3y_4 \\
a_3 = x_1y_2z_4 + x_4y_1z_2 + x_2y_4z_1 - x_4y_2z_1 - x_1y_4z_2 - x_2y_1z_4 \\
a_4 = x_3y_2z_1 + x_1y_3z_2 + x_2y_1z_3 - x_1y_2z_3 - x_2y_3z_1 - x_3y_1z_2 \\
b_1 = y_3z_2 + y_4z_3 + y_2z_4 - y_3z_4 - y_2z_3 - y_4z_2 \\
b_2 = y_3z_4 + y_1z_3 + y_4z_1 - y_3z_1 - y_1z_4 - y_4z_3 \\
b_3 = y_2z_1 + y_4z_2 + y_1z_4 - y_2z_4 - y_1z_1 - y_4z_1 \\
b_4 = y_2z_3 + y_1z_2 + y_3z_1 - y_2z_1 - y_1z_3 - y_3z_2 \\
c_1 = x_3z_4 + x_2z_3 + x_4z_2 - x_3z_2 - x_2z_4 - x_4z_3 \\
c_2 = x_3z_1 + x_4z_3 + x_1z_4 - x_3z_4 - x_1z_3 - x_4z_1 \\
c_3 = x_2z_4 + x_1z_2 + x_4z_1 - x_2z_1 - x_4z_2 - x_1z_4 \\
c_4 = x_2z_1 + x_1z_3 + x_3z_2 - x_2z_3 - x_1z_2 - x_3z_1 \\
d_1 = x_3y_2 + x_4y_3 + x_2y_4 - x_3y_4 - x_2y_3 - x_4y_2 \\
d_2 = x_3y_4 + x_1y_3 + x_4y_1 - x_3y_1 - x_1y_4 - x_4y_3 \\
d_3 = x_2y_1 + x_4y_2 + x_1y_4 - x_2y_4 - x_1y_2 - x_4y_1 \\
d_4 = x_2y_3 + x_1y_2 + x_3y_1 - x_2y_1 - x_3y_2 - x_1y_3
\end{cases}
$$

$$
\Delta = \pm \begin{vmatrix} 1 & x_1 & y_1 & z_1 \\ 1 & x_2 & y_2 & z_2 \\ 1 & x_3 & y_3 & z_3 \\ 1 & x_4 & y_4 & z_4 \end{vmatrix}
$$

Using the above coefficient in Equation 77 gives:

Element 1:

$N_1 = -3.2 - 0.8x + 2.2y + 6z$

$N_2 = 0.8 - 0.4x + 1.15y - 9z$

$N_3 = -5 - 0.5x - 0.9y + 3z$

$N_4 = -10 + 0.05x$

Element 2:

$N_1 = 5.85 - 0.25x + 0.5x - 6z$

$N_2 = -1.2 - 0.15x + 0.1y + 2z$

$N_3 = -3.2 + 0.2x - 1.4y + 12z$

$N_4 = 2.4 - 0.2x - 8z$

Element 3:

$N_1 = -0.4x - 0.4y + 8z$

$N_2 = 0.6x - 0.6y - 12z$

$N_3 = -0.3x + 1.3y - 4z$

$N_4 = -2.4 + 0.2x - 0.4y + 8z$

The matrices [P], [H] at [F] are calculated using the respective values and Equation 79:

For element 1:

$$[H]_1 = \frac{1}{759.6}\left\{\begin{vmatrix} 0.64 & 0.32 & 0.4 & -0.04 \\ 0.32 & 0.16 & 0.2 & -0.02 \\ 0.4 & 0.2 & 0.25 & -0.025 \\ -0.04 & -0.02 & -0.025 & 0.0025 \end{vmatrix} + \begin{vmatrix} 4.84 & 2.53 & -1.98 & 0 \\ 2.53 & 1.3225 & -1.035 & 0 \\ -1.98 & -1.035 & 0.81 & 0 \\ 0 & 0 & 0 & 0 \end{vmatrix} + \begin{vmatrix} 36 & -54 & 18 & 0 \\ -54 & 81 & -27 & 0 \\ 18 & -27 & 9 & 0 \\ 0 & 0 & 0 & 0 \end{vmatrix}\right\} =$$

$$= \frac{1}{759.6}\begin{vmatrix} 41.48 & -51.15 & 16.42 & -0.04 \\ -51.15 & 82.4825 & -27.835 & -0.02 \\ 16.42 & -27.835 & 10.06 & -0.025 \\ -0.04 & -0.02 & -0.025 & 0.0025 \end{vmatrix} = \begin{vmatrix} 0.054 & -0.067 & 0.02 & -5.26e-5 \\ -0.067 & 0.11 & 0.036 & -2.63e-5 \\ 0.02 & 0.036 & 0.013 & -3.29e-5 \\ -5.26e-5 & -2.63e-5 & -3.29e-5 & 3.29e-6 \end{vmatrix}$$

$$[P]_1 = \begin{vmatrix} 195.4 & -1741 & -568.4 & -146.7 \\ -1741 & 26.42 & -1059 & 65.5 \\ -568.4 & -1059 & 913.7 & 279.3 \\ -146.7 & 65.5 & 279.3 & 674.5 \end{vmatrix}$$

$$[F]_1 = \frac{m_1 c_p \Delta T_1 \Delta_1}{4} = \begin{bmatrix} 768.15 \\ 768.15 \\ 768.15 \\ 768.15 \end{bmatrix}$$

For element 2:

$$[H]_2 = \frac{1}{180}\left\{\begin{vmatrix} 0.063 & 0.037 & -0.05 & 0.05 \\ 0.037 & 0.023 & -0.03 & 0.03 \\ -0.05 & -0.03 & 0.04 & -0.04 \\ 0.05 & 0.03 & -0.04 & 0.04 \end{vmatrix} + \begin{vmatrix} 0.25 & 0.05 & -0.7 & 0 \\ 0.05 & 0.01 & -0.14 & 0 \\ -0.7 & -0.14 & 1.96 & 0 \\ 0 & 0 & 0 & 0 \end{vmatrix} + \begin{vmatrix} 36 & -12 & -72 & 48 \\ -12 & 4 & 24 & -16 \\ -72 & 24 & 144 & -96 \\ 48 & -16 & -96 & 64 \end{vmatrix}\right\} =$$

$$= \frac{1}{180}\begin{vmatrix} 36.313 & -11.913 & -72.75 & 48.05 \\ -11.913 & 4.033 & 23.83 & -15.97 \\ -72.75 & 23.83 & 146 & -96.04 \\ 48.05 & -15.97 & -96.04 & 64.04 \end{vmatrix} = \begin{vmatrix} 0.2 & -0.06 & -0.4 & 0.26 \\ -0.06 & 0.02 & 0.13 & -0.089 \\ -0.4 & 0.13 & 0.81 & -0.53 \\ 0.26 & -0.089 & -0.53 & 0.35 \end{vmatrix}$$

$$[P]_2 = \begin{vmatrix} 48.48 & 3.21 & 185.8 & -23.62 \\ 3.21 & 4.727 & 1.19 & 8.1 \\ 185.8 & 1.19 & -12.27 & 211.7 \\ -23.62 & 8.1 & 211.7 & 0 \end{vmatrix}$$

$$[F]_2 = \frac{m_2 c_p \Delta T_2 \Delta_2}{4} = \begin{bmatrix} 754.67 \\ 754.67 \\ 754.67 \\ 754.67 \end{bmatrix}$$

And for element 3:

$$[H]_3 = \frac{1}{172.8}\left\{\begin{vmatrix} 0.16 & -0.24 & 0.12 & 0.05 \\ -0.24 & 0.36 & -0.18 & 0.12 \\ 0.12 & -0.18 & 0.09 & -0.06 \\ 0.05 & 0.12 & -0.06 & 0.04 \end{vmatrix} + \begin{vmatrix} 0.16 & 0.24 & -0.52 & 0.16 \\ 0.24 & 0.36 & -0.78 & 0.24 \\ -0.52 & -0.78 & 1.69 & -0.52 \\ 0.16 & 0.24 & -0.52 & 0.16 \end{vmatrix} + \begin{vmatrix} 64 & -96 & -32 & 64 \\ -96 & 144 & 48 & -96 \\ -32 & 48 & 16 & -32 \\ 64 & -96 & -32 & 64 \end{vmatrix}\right\} =$$

$$= \frac{1}{172.8}\begin{vmatrix} 64.32 & -96 & -32.4 & 64.21 \\ -96 & 144.72 & 47.14 & -95.64 \\ -32.4 & 47.14 & 17.78 & -32.58 \\ 64.21 & -95.64 & -32.58 & 64.2 \end{vmatrix} = \begin{vmatrix} 0.37 & -0.55 & -0.18 & 0.37 \\ -0.55 & 0.84 & 0.27 & -0.55 \\ -0.18 & 0.27 & 0.1 & 0.19 \\ 0.37 & -0.55 & 0.19 & 0.37 \end{vmatrix}$$

$$[P]_3 = \begin{vmatrix} 16.48 & -10.75 & -1.464 & 7.17 \\ -10.75 & 22.51 & -8.85 & 24.47 \\ -1.464 & -8.85 & -137.3 & 1.014 \\ 7.17 & 24.47 & 1.014 & 2.624 \end{vmatrix}$$

$$[F]_3 = \frac{m_3 c_p \Delta T_3 \Delta_3}{4} = \begin{bmatrix} 741.19 \\ 741.19 \\ 741.19 \\ 741.19 \end{bmatrix}$$

The generalized matrixes are:

$$[H]_g = \begin{vmatrix} 0.054 & -0.06 & -0.4 & 5.26e-5 & 0 & 0 \\ -0.06 & 0.22 & 0.07 & -4e-1 & 0.26 & 0 \\ -0.4 & 0.07 & 1.2 & -4.2e-1 & -0.269 & 0.37 \\ 5.26e-5 & -4e-1 & -4.2e-1 & 1.65 & -0.26 & -0.55 \\ 0 & 0.26 & -0.269 & -0.26 & 0.45 & 0.19 \\ 0 & 0 & 0.37 & -0.55 & 0.19 & 0.37 \end{vmatrix} [P]_g = \begin{vmatrix} 195.4 & -1741 & -568.4 & -1.47e2 & 0 & 0 \\ -1741 & 74.9 & -1055.79 & 2.51e2 & -26.32 & 0 \\ -568.4 & -1055.79 & 934.907 & 2.7e2 & 6.636 & 7.17 \\ -1.47e2 & 2.51e2 & 2.7e2 & 6.85e2 & 202.85 & 24.47 \\ 0 & -26.32 & 6.636 & 202.85 & -137.3 & 1.014 \\ 0 & 0 & 7.17 & 24.47 & 1.014 & 2.624 \end{vmatrix}$$

$$[F]_f = \begin{Bmatrix} 768.15 \\ 1522.82 \\ 2264.01 \\ 2264.01 \\ 1495.86 \\ 741.19 \end{Bmatrix}$$

The problem consists of modelling one element with the dimensions 10x10x5 km. The grid shown in Figure 2 will be used.

Now it will be shown how to practically solve the equation for the unstable temperature field using finite volumes:

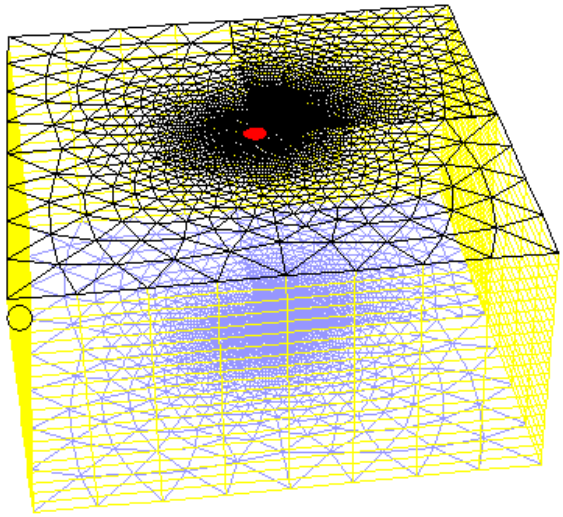

FIGURE 2: The grid

$$\frac{\partial}{\partial x}(k_x \frac{\partial T}{\partial x}) + \frac{\partial}{\partial y}(k_y \frac{\partial T}{\partial y}) + \frac{\partial}{\partial z}(k_z \frac{\partial T}{\partial Z}) + q(x,y,z) - c\frac{\partial T}{\partial t} = 0$$

The software FLUENT was used to obtain results. The results for the temperature, density and velocity distributions are shown in the Figures below.

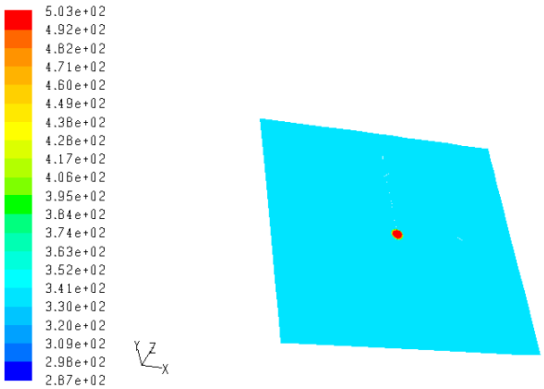

FIGURE 3: The temperature at the bottom

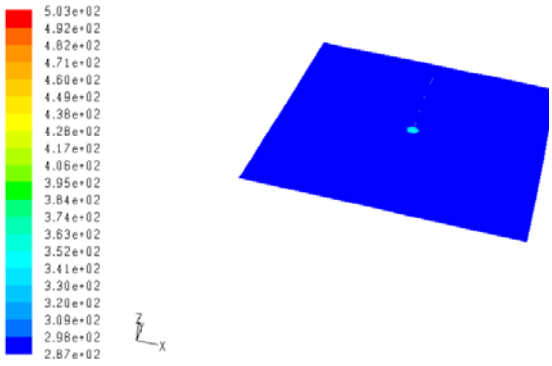

FIGURE 4: The temperature on the surface

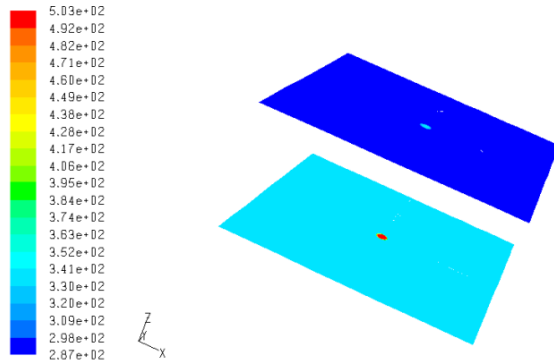

FIGURE 5: The temperature distribution

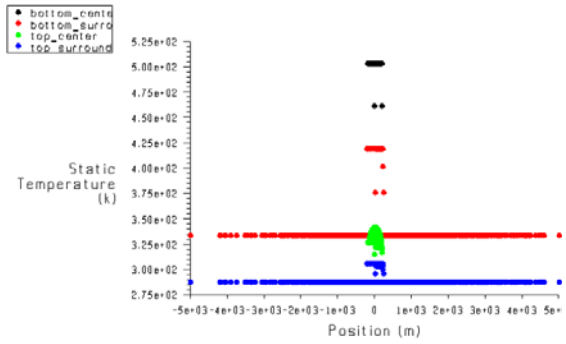

FIGURE 6: The temperature magnitude

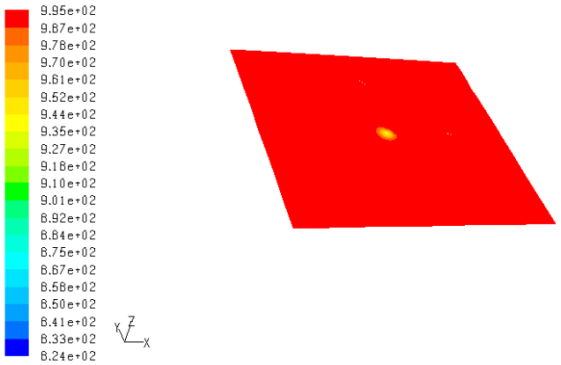

FIGURE 7: The density at the bottom

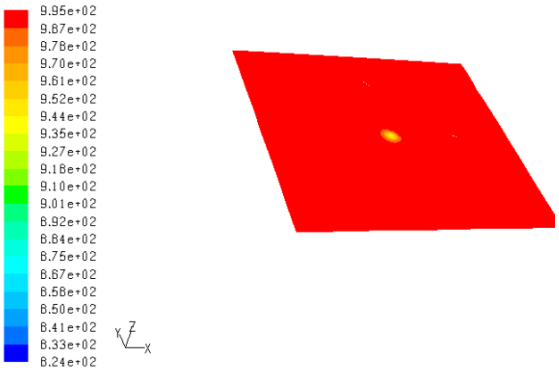

FIGURE 8: The density on the surface

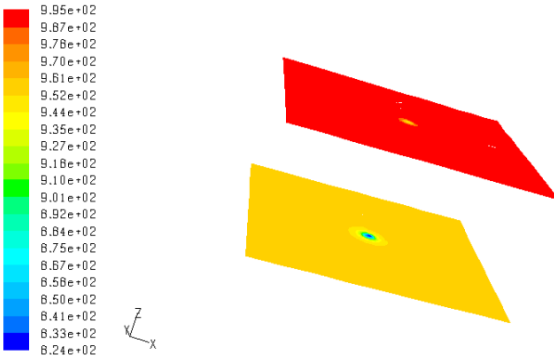

FIGURE 9: The density distribution

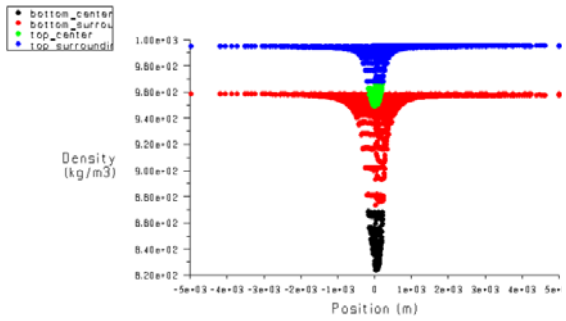

FIGURE 10: The density magnitude

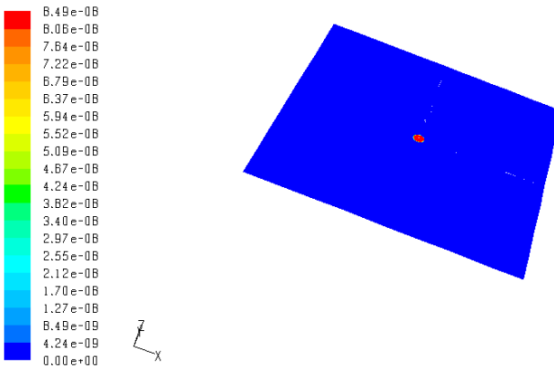

FIGURE 11: The velocity at the bottom

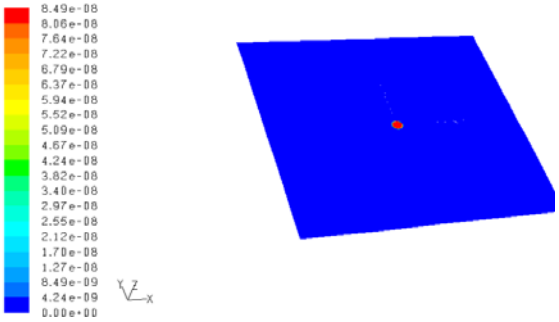

FIGURE 12: The velocity on the surface

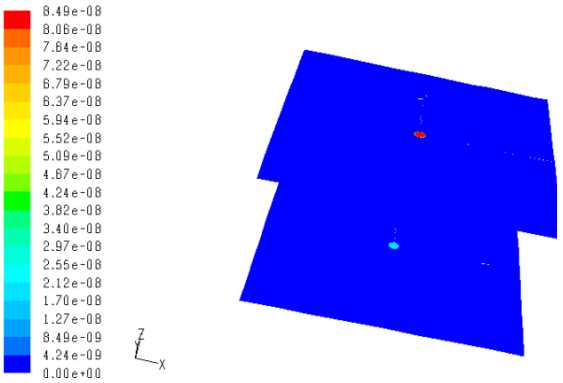

FIGURE 13: The velocity distribution

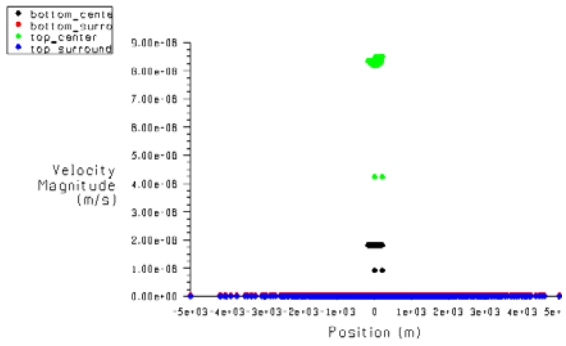

FIGURE 14: The velocity magnitude

APPENDIX II: Calculations for the Llixha-Elbasan-Albania network system.

d_o_1	d_o_2	l_bend_1	l_bend_2	l_v_1	l_v_2	L_equivalent_1	L_equivalent_2	L_equivalent
0.073	0.02667	1.46	0.5334	0.73	0.2667	2079	3549	5628
0.0889	0.0733	1.778	1.466	0.889	0.733	2096	3634	5730
0.1016	0.0889	2.032	1.778	1.016	0.889	2110	3663	5772
0.1143	0.1016	2.286	2.032	1.143	1.016	2123	3686	5809

delta_1	delta_2	d_i_1	d_i_2	A_1	A_2	v_hotwater_1	v_hotwater_2	R_e_1
0.002108	0.001651	0.06878	0.02337	0.003716	0.000429	5.382	46.63	841395
0.002108	0.002108	0.08468	0.06908	0.005632	0.003748	3.551	5.336	683417
0.002108	0.002108	0.09738	0.08468	0.007448	0.005632	2.685	3.551	594292
0.002108	0.002108	0.1101	0.09738	0.009518	0.007448	2.101	2.685	525732

R_e_2	f_1	f_2	H_f_1	H_f_2	P_hidrostatic	p_consumer	P_pumping	DELTAh_pump
2.48E+06	0.01192	0.0091	0.05117	14.74	4.808	2.31	8.54	88.81
837741	0.01256	0.01193	0.01921	0.08763	4.808	2.31	7.128	74.13
683417	0.013	0.01256	0.009958	0.03357	4.808	2.31	7.122	74.07
594292	0.01341	0.013	0.005599	0.0174	4.808	2.31	7.12	74.05

P_motor	price_electricity	C_electricity	C_electricity_annual	price_pipes_1	price_pipes_2	C_pipes_1	C_pipes_2	C_pipes
22326	0.07	1.563	13691	4.2	3.9	8400	13650	22050
18636	0.07	1.304	11427	4.5	4.2	9000	14700	23700
18620	0.07	1.303	11418	4.8	4.5	9600	15750	25350
18615	0.07	1.303	11414	5	4.8	10000	16800	26800

pr_bend_1	pr_bend_2	C_bends_1	C_bends_2	C_bends	pr_junc_1	pr_junc_2	C_junctions_1	C_junctions_2
2.45	1.89	61.25	82.69	143.9	1.8	1.38	48.6	63.14
2.9	2.15	72.5	94.06	166.6	2.1	1.59	56.7	72.74
3.54	2.45	88.5	107.2	195.7	2.34	1.8	63.18	82.35
3.82	2.9	95.5	126.9	222.4	2.52	2.1	68.04	96.08

C_junctions	C_valves_1	C_valves_2	C_valves	pr_pump	C_pump	C_capital	C_operativ	C_total
111.7	158	129	287	1250	1250	22593	14367	36960
129.4	174	136	310	1500	1500	24306	11992	36298
145.5	202	158	360	1670	1670	26051	11982	38033
164.1	230	174	404	2010	2010	27590	11979	39569

R_m	R_p_c	R_p_h	S	Sc	Sh	f_c	S_allowabl	y
340	235	140	93.33	113.3	93.33	1	165	0.4
410	275	165	110	136.7	110	0.9	178.5	0.5
490	355	195	130	163.3	130	0.8	189.3	0.7
540	405	215	143.3	180	143.3	0.7	182.6	0.7

th_presclass_1	th_presclass_2	d_i_1_c	d_i_2_c	d_average	Z_1	Z_2	q_pipe_1	q_pipe_2
2.901	1.726	0.0672	0.02322	0.04521	1.08E05	7.93E07	49180	10414
2.79	2.485	0.08332	0.06833	0.07582	1.58E05	9.47E06	58111	42559
2.912	2.679	0.09578	0.08354	0.08966	2.17E05	1.52E05	69502	55868
3.219	2.978	0.1079	0.09564	0.1018	3.04E05	2.21E05	86491	71041

q_pipe_total	d_ins_1	d_ins_2	q_insulation_1	q_insulation_2	q_ins_total	q_sust_vertical	v_win	q_wind_1
59593	0.083	0.03667	9973	4049	14022	73616	4	498
100670	0.0989	0.0833	12006	10011	22017	122688	5	927.2
125370	0.1116	0.0989	13630	12006	25636	151006	6	1507
157532	0.1243	0.1116	15254	13630	28884	186416	7	2284

q_wind_2	q_wind_total	q_water_1	q_water_2	q_water_total	q_0	q_seismic	q_d_h	q_medium_1
220	718	70894	14447	85342	158958	38150	38150	34781
780.9	1708	109890	128145	238035	360723	86573	86573	53471
1335	2842	146156	193054	339210	490216	117652	117652	70655
2051	4335	186571	254641	441213	627628	150631	150631	89610

q_medium_2	q_medium_total	q_snow_1	q_snow_2	q_snow_total	q_seismic_vertical	q_d_v	M_A	M_B
4152	38933	19.92	8.801	28.72	19075	58037	2.91E+11	2.75E+11
35963	89434	23.74	19.99	43.73	43287	132764	5.04E+11	6.51E+11
53757	124411	26.78	23.74	50.52	58826	183288	6.29E+11	9.07E+11
70459	160069	29.83	26.78	56.62	75315	235441	7.86E+11	1.18E+12

L_supports_1	L_supports_2	DELTAL_1	DELTAL_2	DELTAL	sigma_x_1	sigma_x_2	Force_1	Force_2
49.93	3.676	1.621	2.768	4.39	1.56E+08	1.56E+08	652920	87149
43.81	26.32	1.635	2.835	4.47	1.56E+08	1.56E+08	968318	658298
54.25	38.05	1.646	2.857	4.502	1.56E+08	1.56E+08	1.27E+06	968318
66.36	48.34	1.656	2.875	4.531	1.56E+08	1.56E+08	1.60E+06	1.27E+06

L_arm_1	L_arm_2	H_tank	V_tank	D_tank	A_tank	H_tank_rm	D_tank_rm	A_tank_rm
2.986	1.805	4	400	11.28	341.8	7.986	7.986	300.5
3.295	2.992	6	600	11.28	412.7	9.142	9.142	393.8
3.523	3.295	8	800	11.28	483.6	10.06	10.06	477.1
3.736	3.523	9	1000	11.89	558.5	10.84	10.84	553.6

P_tank_abs	e_tank_min	e_a	sigma_b_c	sigma_b_a	e_roof
1.643	7.298	6.248	1.85E+08	1.54E+07	5.087
1.754	8.685	7.635	1.97E+08	1.64E+07	5.823
1.842	9.878	8.828	2.07E+08	1.72E+07	6.409
1.917	10.95	9.895	2.15E+08	1.79E+07	6.904

APPENDIX III: Results of calculations for heat exchangers

m	T_r	Q_hotwater	m_o	T_r_o	Q_hotwater_o	eta_hotwater	T_i	T_i_o
3.92	30	491.6	17.64	33	2360	0.2083	18	18.5
4.9	33	553	19.6	35	2458	0.225	18.5	19
5.88	36	589.9	21.56	38	2433	0.2424	19	19.4
6.86	40	573.5	23.52	40	2458	0.2333	19.8	20

eta_radiator	T_o	T_o_0	k_l	Q_loss_building	eta_building	tau	U_p	tau_o
0.8331	4	6.7	93.63	2060	0.873	0.9474	0.8859	0.9881
0.8739	5	8	91.03	2139	0.8704	0.9474	1.107	0.9866
0.8759	6	9	85.68	2142	0.8803	0.9474	1.329	0.9854
0.9243	10	13.5	73.37	2186	0.8896	0.9474	1.55	0.9844

T_s_h	T_s_h_r	T_rwater	T_rwater_r	Q_building_capacity	m_o_r
60	60	28.74	28.74	6.137	16.43
60	60	31.58	31.58	6.905	18.95
60	60	34.42	34.42	7.366	21.35
60	60	38.21	38.21	7.161	26.15

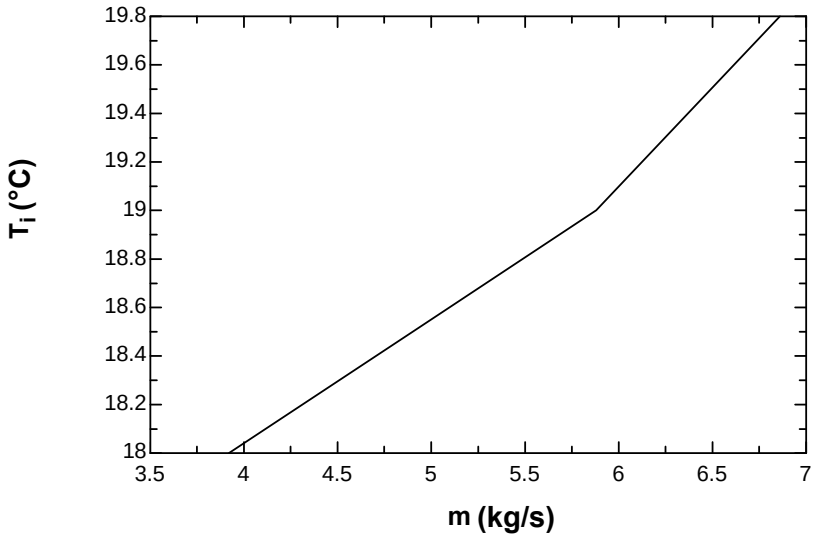

FIGURE 1: The indoor temperature

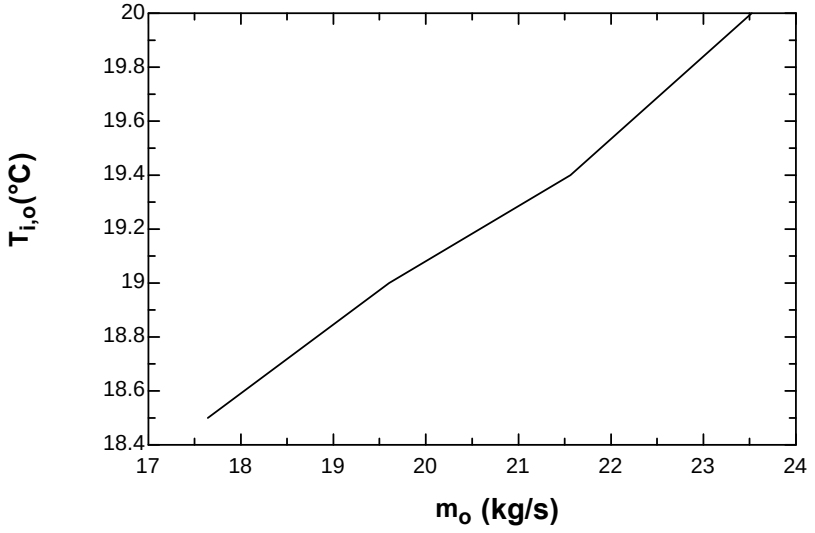

FIGURE 2: The reference indoor temperature